Multi-objective periodic railway timetabling on dense heterogeneous railway corridors

Yan, Fei; Bešinović, Nikola; Goverde, Rob

DOI
10.1016/j.trb.2019.05.002

Publication date
2019

Document Version
Accepted author manuscript

Published in
Transportation Research Part B: Methodological

Multi-objective periodic railway timetabling on dense heterogeneous railway corridors

Fei Yan*, Nikola Bešinović, Rob M.P. Goverde

Department of Transport and Planning, Delft University of Technology, P.O.Box 5048, 2600GA Delft, The Netherlands

Abstract

This paper proposes a new multi-objective periodic railway timetabling (MOPRT) problem with four objectives to be minimized: train journey time, timetable regularity deviation, timetable vulnerability and the number of overtakings. The aim is to find an efficient, regular and robust timetable that utilizes the infrastructure capacity as good as possible. Based on the Periodic Event Scheduling Problem, we formulate the MOPRT problem as a Mixed Integer Linear Program (MILP). The ε-constraint method is applied to deal with the multi-objective property, and algorithms are designed to efficiently create the Pareto frontier. By solving the problem for different values of ε, the four-dimensional Pareto frontier is explored to uncover the trade-offs among the four objectives. The optimal solution is obtained from the Pareto-optimal set by using standardized Euclidean distance, while capacity utilization is used as an additional indicator to chose between close solutions. Computational experiments are performed on a theoretical instance and a real instance in one direction of a Dutch railway corridor, demonstrating the efficiency of the model and approach.

Keywords: Periodic timetable, multi-objective optimization, timetable robustness, flexible overtaking, ε-constraint

1. Introduction

With the growth of passenger demand, the operation of a rail transport system becomes a complex problem and highly challenging in busy and dense networks. In order to provide an attractive railway system, short travel times from origins to destinations are desired by passengers, while the vulnerability of dense traffic to delays also requires more emphasis on timetable robustness. Moreover, in busy corridors, passengers prefer having the possibility to travel without the need of checking the timetable, but expect to find a train service at regular intervals. This asks for more regular operations equally distributed in time. Meanwhile, heterogeneous traffic with different train types (with different speed profiles) and different stop patterns to meet the demand in railway operation, make it more complex than metro systems. In order to provide a high-performance service, railway train operations must be carefully planned and consider all these aspects when designing timetables. However, these multiple objectives are sometimes opposite, and difficult to be handled by planners simultaneously.

The periodic railway timetabling problem aims at optimizing departure and arrival times at each station of every train from a given line plan ($\mathcal{L}$) consisting of lines with their stop patterns (l) and the corresponding frequency (f_l) for a timetable period length T. So far, different performance indicators have been introduced, generally including timetable efficiency, feasibility, infrastructure (capacity) occupation, stability, robustness and energy consumption (Goverde et al., 2016). Timetable efficiency is measured by the scheduled journey time including running times, dwell times and transfer times between any two stations, while capacity occupation is the share of time required to operate trains on a given railway infrastructure according to a given timetable pattern (Goverde and Hansen, 2013). Timetable robustness has many different interpretations and definitions, but most measures are related to the distribution of buffer times (Lusby et al., 2018). There are two types of methods that are typically used to assess the level of robustness.

*Corresponding author

Email addresses: f.yan@tudelft.nl (Fei Yan), N.Besinovic@tudelft.nl (Nikola Bešinović), r.m.p.goverde@tudelft.nl (Rob M.P. Goverde)

One is to measure the defined performance indicators for a fixed timetable (Peeters, 2003; Bešinović, 2017; Yan and Goverde, 2017), and the other is to simulate the timetable with different (delay) scenarios and assess it with a proposed objective (Kroon et al., 2008; Liebchen et al., 2009; Bešinović et al., 2016; Maróti, 2017). In the macroscopic planning level, robustness can be interpreted as the ability of a timetable to resist delays. Increasing the buffer time between two trains helps a timetable to absorb certain disturbances or reduce the propagation of delays to other trains.In addition, service regularity means that trains from the same line depart at regular intervals at each station along the path, which could help to attract more passengers. To address all relevant indicators, timetabling models (Kroon and Peeters, 2003; Peeters, 2003; Liebchen, 2007) with objectives of passenger travel time and train journey time only are not sufficient anymore. Timetable robustness can be enhanced by allocating so-called buffer times between train paths above the minimal headway times to absorb some disturbances and prevent the delay propagation to the following trains, where a balanced buffer time distribution provides better timetable robustness. For a given infrastructure and line plan, capacity utilization is usually computed as an ex-ante indicator and not part of timetable optimization. It can be used to compare the quality of the timetables or evaluate the possibility to add more trains. Timetable efficiency, robustness, and regularity are straightforwardly related to the level of service to passengers and can be enhanced during the planning process. Therefore, multiple objectives need to be taken into account when designing timetables to improve the overall quality of the railway transport system.

Train overtakings affect timetable robustness and capacity utilization and are in particular useful when different train speeds exist on the same corridor, as illustrated in Figure 1. Here, we assume that the station capacity is enough as overtakings require additional station track capacity. All sub-figures contain two lines l_1 and l_2 with frequency two in one period pattern at four stations. Here the minimum cycle time (λ_a and λ_b) (Goverde, 2007) is applied to represent timetable capacity utilization for the given line plan. Figure 1(a) depicts a compressed timetable pattern with strict regularity constraints, minimum arrival/departure headway and the minimum cycle time (equals period length) $\lambda_a = T$, when overtakings are not allowed. Figure 1(b) shows a compressed timetable with the minimum cycle time λ_b with the minimum headway constraints when overtakings are allowed. It can be seen that the latter has a lower capacity utilization by comparison of λ_a and λ_b ($\lambda_a > \lambda_b$). Figure 1(c) shows the same timetable pattern as Figure 1(b), but includes buffer times to reach the same period length as Figure 1(a). Hence, the robustness is better than the one in Figure 1(a) although with some travel time loss.

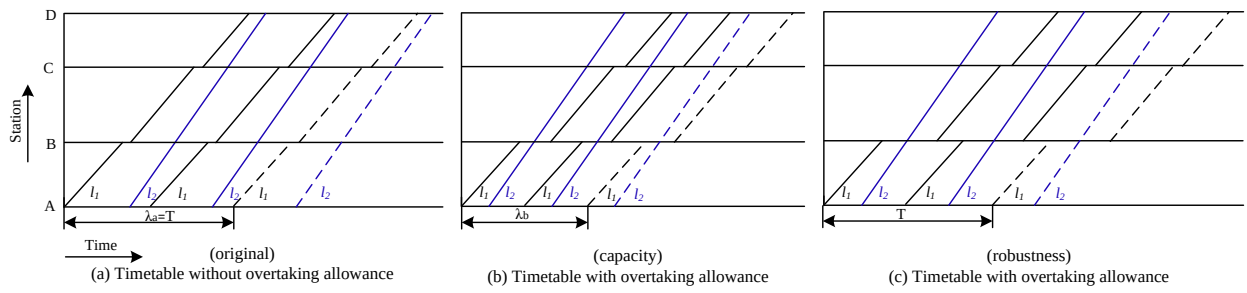

Figure 1: Timetable layouts with and without overtakings: (a) original timetable when overtakings are not allowed (b) capacity utilization when overtakings are allowed; (c) Timetable robustness when overtakings are allowed

In general, overtakings could help to improve timetable robustness and reduce capacity utilization, but too many overtakings would lead to an increase of train journey time. Also the maximum number of overtakings due to the station capacities must be considered. Therefore, it is important to keep track of the number of overtakings and control them during timetable construction by balancing their effect on timetable journey times, robustness and capacity. To this aim, we introduce the concept of flexible overtaking.

Flexible overtaking represent that a train can be overtaken (i) by more than one train at each station; (ii) multiple times along its path; (iii) at any station along its path. In particular, flexible overtaking allow finding the best overtaking locations for an existing rail network. For instance, local trains may be overtaken by Intercity or/and International trains at several stations, and freight trains are overtaken by passenger trains multiple times at one station.

The Periodic Event Scheduling Problem (PESP) (Serafini and Ukovich, 1989) is a feasibility problem that has been successfully applied to model the macroscopic scheduling of a periodic timetable in rail networks, usually including an

additional objective function to turn the feasibility problem into an optimization problem (Nachtigall, 1996; Peeters, 2003; Liebchen and Möhring, 2007). Peeters (2003) presented several objectives from passenger and operator aspects, and solved them by setting up a Mixed Integer Linear Programming (MILP). Illegal overtakings (conflicts) when two trains occupy the same open track section at the same time may occur when variable trip times (constrained by a lower and upper bound) are set in the model. To address this issue, extra dummy nodes are adopted to forbid the conflicts in Kroon and Peeters (2003) and Sparing and Goverde (2017), while a relation of modulo parameters is presented to find a conflict-free timetable in Zhang and Nie (2016). Both optimization models in Sparing and Goverde (2017) and Zhang and Nie (2016) designed overtaking constraints with allowance of at most one overtaking at each dwell activity, while multiple overtakings have not been modeled in the literature so far. Parbo et al. (2016) reviewed the train-oriented and passenger-oriented timetabling models on different aspects, and put forward guidelines to narrow the gap between operators' railway planning and passengers' perception of the railway performance, especially regarding robustness.

A lot of achievements have been obtained in robust timetable optimization to reduce delay propagation. A robustness objective function is proposed in Peeters (2003) by pulling apart trains, that is, to push the headway to half the cycle time to increase overall buffer times at all stations. This procedure is optimizing at the same time train orders and event times, but it is quite difficult to achieve the optimal solution for real-life cases. For most other research, the aim is to optimize an existing and feasible timetable to improve its robustness against delays or disturbances, such as stochastic programming in Kroon et al. (2008), recoverable robustness in Liebchen et al. (2009) and a branch-and-bound method in Maróti (2017). Bešinović et al. (2016) proposed an integrated approach combining the microscopic and macroscopic level of timetable design to improve timetable robustness, and the objective for robustness cost is the delay settling time using Monte Carlo simulation. Goverde et al. (2016) extended this approach to include a third level to optimize energy efficient train operation. Based on the model in Sparing and Goverde (2017), Bešinović (2017, Chapter 5) proposed a two-stage model to achieve a stable and robust timetable. The first stage finds the optimal stable timetable structure by minimizing capacity utilization and journey times, while the second stage improves timetable robustness by optimizing the allocation of time allowances. Sels et al. (2016) presented a MILP approach to find robust timetables while minimizing the total expected passenger travel time, and applied it to the Belgium railway network with all hourly passenger trains. Yan and Goverde (2017) compared several periodic timetable optimization models, and gave a number of performance indicators to assess robustness. Two recent reviews on timetabling models in different railway planning stages can be found in Caimi et al. (2017) and Lusby et al. (2018).

In this paper, we propose a multi-objective periodic railway timetabling (MOPRT) optimization model, which aims to find an efficient, regular and robust timetable that utilizes the infrastructure capacity as good as possible. Based on the Periodic Event Scheduling Problem, we formulate the MOPRT problem as a Mixed Integer Linear Program (MILP). Train journey time is introduced to minimize travel time in order to improve transport system efficiency. Timetable regularity provides regular train services for passengers, and the corresponding objective tries to minimize the regularity deviation. To incorporate robustness, *timetable vulnerability* is proposed based on a new piecewise linear headway penalty function. It is designed to step away from too small headways and too big headways due to periodicity in the timetable, so minimization of timetable vulnerability leads to a balanced distribution of buffer times at stations. Meanwhile, the number of overtakings may increase while enhancing the overall robustness of the timetable, especially in a dense corridor. Thus, we minimize the number of overtakings using flexible overtaking constraints to obtain the best overtaking locations. To deal with the multi-objective property of our model, the ε-constraint method is introduced to explore the Pareto frontier. Three algorithms are designed to speed up the computation by reducing the search space to efficiently create the Pareto frontier. The trade-offs among the four objectives are analyzed to uncover the correlations between each other. Standardized Euclidean distance is used to find the optimal solution from the Pareto-optimal, while the minimum cycle time is used to evaluate the resulting capacity utilization for the timetables.

The main contributions of this paper are as follows:

- A multi-objective periodic timetable model is developed that optimizes train journey time, regularity deviation, timetable vulnerability and the number of overtakings.
- A new timetable vulnerability objective with related constraints is formulated based on a piecewise headway penalty to improve timetable robustness.
- Flexible overtaking objective and constraints are designed to find the best overtaking locations and number of overtakings.

- An ε-constraint method is introduced to explore the Pareto frontier for the multi-objective model, and analyze the trade-offs between all objectives.
- The approach is demonstrated in a theoretical instance and a real-world Dutch railway corridor.

The paper is organized as follows: Section 2 presents the model formulations of the four objectives and corresponding constraints for periodic railway timetabling optimization. Section 3 introduces the approach to deal with multiple objectives and describes the indicator of capacity utilization. Section 4 illustrates the approach with experiments and computational results both in the theoretical instance and the real world case, and finally Section 5 summaries the paper with main findings and conclusions.

2. Model Description

2.1. Periodic event activity network

The PESP formulation is represented by a direct graph $\mathcal{G} = (\mathcal{E}, \mathcal{A}, T)$, which represents a periodic event-activity network, as shown in Figure 2. A given line plan is defined with a set of lines $\mathcal{L}$ and stations $\mathcal{S}$. Each line $l \in \mathcal{L}$ defines a stopping pattern $(s_1, .., s_k, .., s_{N_l})$, $s_k \in \mathcal{S}$ and a frequency f_l within a given time period length T.

The set $\mathcal{E}$ contains departure events $\mathcal{E}(s_1)$ at start station s_1, arrival and departure events (for a stop station) or arrival-through and departure-through events (for a non-stop station) $\mathcal{E}(s_k)$ at s_k, and arrival events $\mathcal{E}(s_N)$ at s_N for all train lines. Note that we use two events generating a through activity for a non-stop station instead of one through event, as this simplifies the model formulation of flexible overtaking. The set of activities $\mathcal{A}$ represents dependencies between pairs of events. For each event i, we determine the scheduled time $\pi_i \in [0, T)$ in a basic period while satisfying the set of activities $\mathcal{A}$. Due to periodicity, one event would occur at times $\pi_i + z \cdot T$, where $z = ... -2, -1, 0, 1, 2, ...$ Each activity time a_{ij} corresponds to an activity $(i, j) \in \mathcal{A}$, where i and j are two consecutive events, which can be distinguished as running time, dwell time, headway time, and regularity interval, and each of them has a lower bound l_{ij} and an upper bound u_{ij}.

Running activities $\mathcal{A}_{\text{run}}$ and dwell activities $\mathcal{A}_{\text{dwell}}$ are generated from the consecutive events of the same train. To allow flexible overtakings, dwell time is taken as a variable. In the PESP literature running times are mostly assumed to be fixed, i.e., having equal lower and upper bounds. But for a dense and heterogeneours corrisor, keeping the running time fixed leads easily to infeasibility. By relaxing the running times to intervals solutions become possible that are not available when considering intervals to dwell times only. Moreover, running time supplements can actually be used in a positive way to recover from delays or energy-efficient driving, while increasing dwell times also leads to increased capacity occupation of platform tracks. The lower bound for running time is the minimum running time, which equals the technical running time plus a minimal time supplement that covers various train behaviors. The upper bound is the maximum running time that can be accepted by passengers and operator. The minimum time for boarding and alighting of passengers, and the maximum time for passengers waiting at stations or the minimal time needed for overtakings represent the lower bound and upper bound of the dwell time. Through activities $\mathcal{A}_{\text{thru}}$ are similar to dwell activities which are also from the same train at the same station, but without time consumption at stations. It represents trains pass through the stations with zero as fixed activity times.

We generate set $\mathcal{A}_{\text{thru}}$ in order to simplify the model design of flexible overtaking. Headway activities $\mathcal{A}_{\text{head}}$ are generated between different train events at the same station. The lower bound l_{ij} for headway time is the minimum (default) time required to avoid conflicting train movements, whilst $T - l_{ji}$ is the upper bound to avoid conflicts between trains in the reverse order. If the frequency f_l of line l is greater than one, regularity activities $\mathcal{A}_{\text{reg}}$ are needed to ensure a regular service. Since all trains from the same train line have the same stop pattern and train type, we predefine a departure sequence of these trains in our model which does not influence the results. Without loss of generality, $\mathcal{A}^l_{\text{reg}}$ represents the regularity activities between trains of line l. The lower and upper bounds are set to be T/f_l to line l when strict regularity is needed. Note that this needs some relaxation if T/f_l is not an integer, which will be discussed later. This ensures regular schedules of line l. Transfer connections and rolling stock connections are not considered in this paper. All activities are represented by $\mathcal{A} = \mathcal{A}_{\text{run}} \cup \mathcal{A}_{\text{dwell}} \cup \mathcal{A}_{\text{thru}} \cup \mathcal{A}_{\text{head}} \cup \mathcal{A}_{\text{reg}}$.

PESP aims at finding event times π_i for all events $i \in \mathcal{E}$, where all activities

$$a_{ij} = \pi_j - \pi_i + z_{ij} \cdot T \tag{1}$$

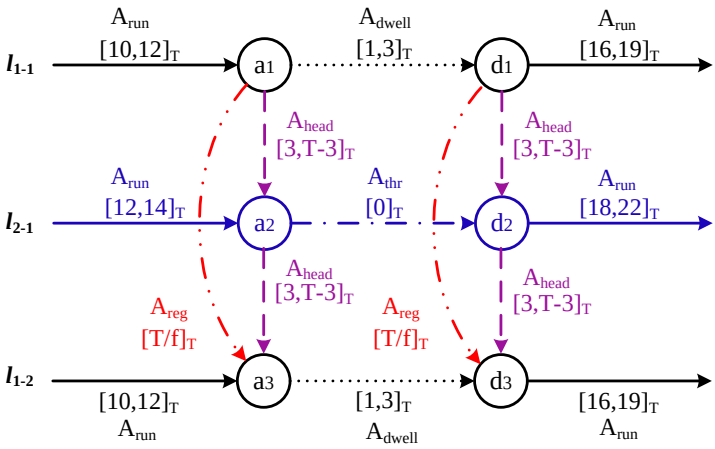

Figure 2: Illustration of a periodic event-activity network for three trains of two lines in a station. Train line l_1 consists of two trains l_{1-1} and l_{1-2}, and train l_{2-1} has a through event at this station. Solid line represents running activities; dotted represents dwell activities; dash-dotted represents through activities; dashed represents headway activities; and dash-double-dotted represents regularity activities. The notation $[l_{ij}, u_{ij}]_T$ is used for the intervals $[l_{ij}, u_{ij}]$ modulo T.

satisfy the lower bound l_{ij} and upper bound u_{ij}. The modulo parameter z_{ij} determines the order of events i and j within a defined time period T, and we assume that $0 \leq l_{ij} \leq u_{ij} \leq T-1$ and $0 \leq u_{ij} - l_{ij} \leq T-1$ If necessary, dummy nodes are introduced to split arcs with $u_{ij} \geq T$ into smaller segments to satisfy these assumptions (Kroon and Peeters, 2003; Sparing and Goverde, 2017). Then $z_{ij} = 1$ if $\pi_i > \pi_j$, and it is 0 otherwise.

2.2. Model formulation

To model a MOPRT problem, we introduce four separate single-objective timetabling optimization models based on the basic PESP. The most common model with the objective of train journey time is presented in Section 2.2.1. To tackle infeasibility or saturated capacity problem by strict regularity, the timetable regularity model is introduced to allow certain regularity deviation within some bound in Section 2.2.2. To improve timetable robustness by increasing buffer times, the timetable vulnerability model is formulated with a specific penalty function in Section 2.2.3. The flexible overtaking model with consideration of multiple overtaking constraints and station capacity while minimizing the number of overtakings is proposed in Section 2.2.4. All of these models will be combined in Section 2.2.5 into a MOPRT model.

2.2.1. Train journey time model (PESP-TJT)

First, we introduce the periodic timetable optimization model *PESP-TJT* with the objective of train journey time, defined as:

$$\text{Minimize} \sum_{(i,j)\in\mathcal{A}_{\text{run}}\cup\mathcal{A}_{\text{dwell}}} \alpha_{ij} \cdot (\pi_j - \pi_i + z_{ij} \cdot T) \tag{2}$$

subject to

$$l_{ij} \leq \pi_j - \pi_i + z_{ij} \cdot T \leq u_{ij} \qquad \forall (i,j) \in \mathcal{A} \tag{3}$$

$$0 \leq \pi_i < T \qquad \forall i \in \mathcal{E} \tag{4}$$

$$z_{ij} \in \{0,1\} \qquad \forall (i,j) \in \mathcal{A} \tag{5}$$

$$z_{ij} + z_{i'j'} + z_{ii'} + z_{jj'} = 2 \cdot c_{ii'jj'} \qquad \forall (i,j),(i',j') \in A_{\text{run}}, (i,i'),(j,j') \in \mathcal{A}_{\text{head}} \tag{6}$$

$$0 \leq c_{ii'jj'} \leq 2 \qquad \forall (i,j),(i',j') \in \mathcal{A}_{\text{run}}, (i,i'),(j,j') \in \mathcal{A}_{\text{head}} \tag{7}$$

$$c_{ii'jj'} \in \mathbb{N}_0 \qquad \forall (i,j),(i',j') \in \mathcal{A}_{\text{run}}, (i,i'),(j,j') \in \mathcal{A}_{\text{head}} \tag{8}$$

Objective function (2) includes train running times and dwell times, and α_{ij} represents the weight of the different activities. Constraint (3) ensures that all activities are within the given bounds. Constraint (4) requires periodicity of events by bounding to $[0, T)$. Constraint (5) restricts the modulo parameters to be binary. The notation $c_{ii'jj'}$ is introduced as an auxiliary integer variable from 0 to 2, and is used to prevent illegal overtaking between running activities (i, j) and (i', j'). Here, activities (i, i') and (j, j') are the corresponding headway activities of two trains at two stations. Constraints (6)-(7) guarantee that no illegal overtaking can arise, when the sum of the four modulo parameters of related running and headway activities equals 0, 2 or 4. This is proposed by Zhang and Nie (2016). Figure 3 illustrates three combinations of modulo parameters between two trains when no illegal overtaking occurs. Variable $c_{ii'jj'}$ is 0 in Figure 3(a) and 1 in Figure 3(b). It becomes 2 in Figure 3(c) when event i' is scheduled earlier than i, and all modulo parameters became 1. In total, there are ten types of timetable situations for two trains without illegal overtaking, and eight types with illegal overtakings, see for details in Zhang and Nie (2016). $\mathbb{N}_0$ in constraint (8) represents the nonnegative integers.

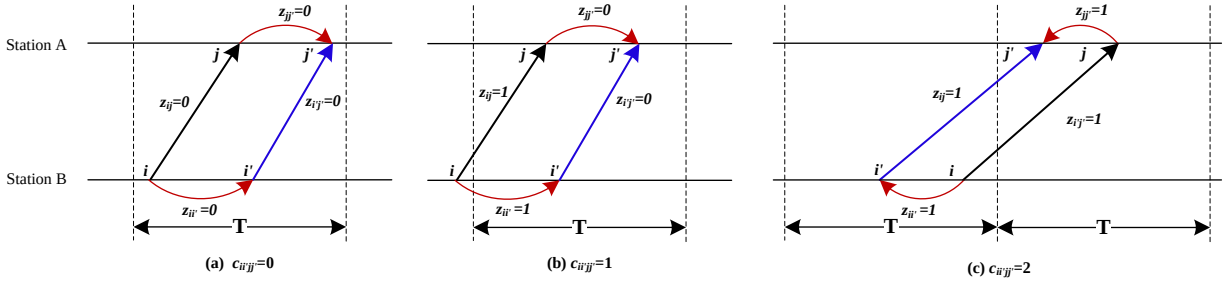

Figure 3: Three combinations of modulo parameters between two trains when no illegal overtaking occurs

2.2.2. *Timetable regularity model (PESP-Reg)*

A strict periodic pattern means that successive trains from the same train line have a regular interval at all stations along their path (only if f_l is a divisor of T), described by T/f_l. However, strict regularity could lead to unnecessary dwell time loss if overtaking occurs. For instance, Figure 4(a) shows two train lines operate in the same corridor from station A to C within period length T. The line l_1 has frequency of two and an all-stop pattern, and line l_2 has frequency one with a non-stop pattern. At station B, activities (i, i') and (j, j') represent dwell activities of trains l_{1-1} and l_{1-2} from the same line l_1, and activity (k, k') is used to represent the dwell activity (i, i') in the following period. Activities (i, j) and (j, k) are the arrival headways of line l_1 at station B, and activities (i', j') and (j', k') are the corresponding departure headways. Under the constraints of strict regularity, both $a_{ij} = a_{jk}$ and $a_{i'j'} = a_{j'k'}$ need to be satisfied. However, this would result to equal dwell times at station B for each train of line l_1, even though there is no overtaking for train l_{1-2}. Figure 4(b) has a smaller dwell time of train l_{1-2} at station B, but the departure interval between trains are not always the same, which gives more flexibility for timetable optimization. This paper proposes a regularity model which can generate timetables like in Figure 4(b).

A variable θ_{ij} is introduced to provide a certain deviation in case T/f_l is not an integer or to express the tolerance from strict regularity, defined as follows (with the notation $\left[\frac{T}{f_l}\right]$ representing rounding to the nearest integer to $\frac{T}{f_l}$).

$$\theta_{ij} = |a_{ij} - \left[\frac{T}{f_l}\right]| \qquad \forall (i, j) \in \mathcal{A}^l_{\text{reg}}, l \in \mathcal{L} \tag{9}$$

In addition, in order to control the deviation range, a new parameter β_l is set as the tolerance upper bound of a line l. Hence, the periodic timetabling model with flexible regularity constraints *PESP-Reg* to minimize the regularity deviation can be modeled as:

$$\text{Minimize} \sum_{(i,j)\in A_{\text{reg}}} \theta_{ij} \tag{10}$$

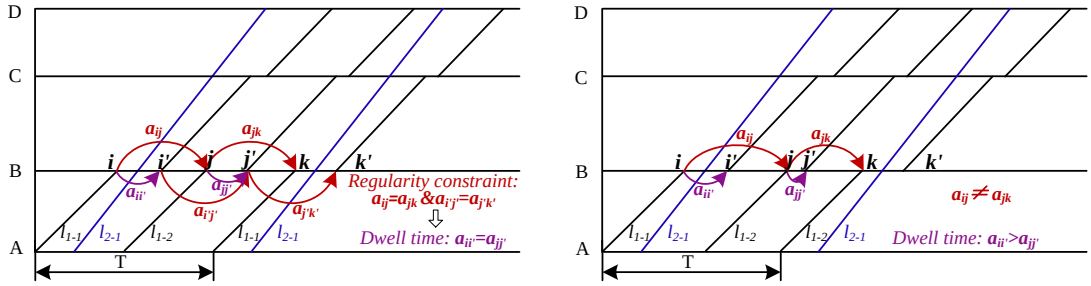

(a) Timetable with strict regularity constraint

(b) Timetable with relaxed regularity constraint

Figure 4: Timetable layouts with (a) strict regularity constraints and (b) relaxed regularity constraints

subject to (3)-(8) and

$$-\theta_{ij} \le a_{ij} - \left\lceil \frac{T}{f_l} \right\rceil \le \theta_{ij} \qquad \forall (i,j) \in \mathcal{A}^l_{\text{reg}}, l \in \mathcal{L} \tag{11}$$

$$0 \le \theta_{ij} \le \beta_l \qquad \forall (i,j) \in \mathcal{A}^l_{\text{reg}}, l \in \mathcal{L} \tag{12}$$

Constraint (11) is the linearized version of equation (9), while strict regularity can also be predefined in this model by setting the corresponding θ_{ij} as 0 if T/f_l is an integer. Constraint (12) ensures that regularity of line l could only deviate within the given tolerance range β_l.

2.2.3. Timetable vulnerability model (PESP-Vnb)

In order to reduce timetable vulnerability, we introduce a penalty function to step away from small headways and big headways. Note that due to the periodicity, big headways are also small headways to the same train in the following period. This is inspired by the idea that pulling apart trains using the same track to enlarge headway times could improve timetable robustness, see Peeters (2003). Apart from the fixed minimum headway time, buffer time in the headway time could mitigate disturbances or delays propagated by other trains. Hence, a robust timetable could be attained with a reasonable distribution of buffer times. A piecewise linear function is designed consisting of three parts: a linear decreasing function to penalize small headways, a constant zero part as no penalty is considered to moderate headways, and a linear increasing function to penalize big headways, see Figure 5. To improve robustness we aim at allocating the buffer times as equal as possible between the events to avoid small buffer times. This reference headway h^p could be generated by:

$$h^p = \left\lceil \frac{T}{N_t} \right\rceil \tag{13}$$

Here, parameter N_t represents the number of trains in the corridor. In addition, we define P_{max} as the maximum penalty value applied to the critical minimum headway times:

$$P_{max} = \phi \cdot (h^p - l^{min}) \tag{14}$$

Here, l^{min} represent the minimum headway and parameter ϕ is the slope of the penalty function. The larger the value of ϕ, the more penalty for small or big headways. For example, if $N_t = 6$, $\phi = 10$ and $l^{min} = 3$ min in the timetable, then $h^p = 60/6 = 10$ min and $P_{max} = 10 \cdot (10 - 3) = 70$. In practice (more generally), various minimum headway times could be used in the timetable design. We therefore determine the minimal headway between all train pairs as $l^{min} = \min_{(i,j)\in\mathcal{A}_{head}} \min(l_{ij}, T - u_{ij})$, which is used in equation (14). Then we introduce a new variable δ_{ij} as the penalty value of activity (i, j) calculated by:

$$\delta_{ij} = \begin{cases} P_{max} - \phi \cdot (a_{ij} - l_{ij}) & a_{ij} \le h_{ij}^{p\_lower} \\ 0 & h_{ij}^{p\_lower} < a_{ij} \le h_{ij}^{p\_upper} \\ P_{max} - \phi \cdot (u_{ij} - a_{ij}) & a_{ij} > h_{ij}^{p\_upper}, \end{cases} \quad \forall (i,j) \in \mathcal{A}_{\text{head}} \tag{15}$$

Parameters $h_{ij}^{p\_lower}$ and $h_{ij}^{p\_upper}$ represent the reference headway value of the lower side and upper side of activity (i, j) due to periodicity. To ensure that the penalty values are the same for two activities with different minimum headways but the same buffer time $h^p - l^{min}$, the lower and upper reference headways are determined for each activity as:

$$h_{ij}^{p\_lower} = l_{ij} + (h^p - l^{min}) \qquad \forall (i,j) \in \mathcal{A}_{\text{head}} \tag{16}$$

$$h_{ij}^{p\_upper} = u_{ij} - (h^p - l^{min}) \qquad \forall (i,j) \in \mathcal{A}_{\text{head}} \tag{17}$$

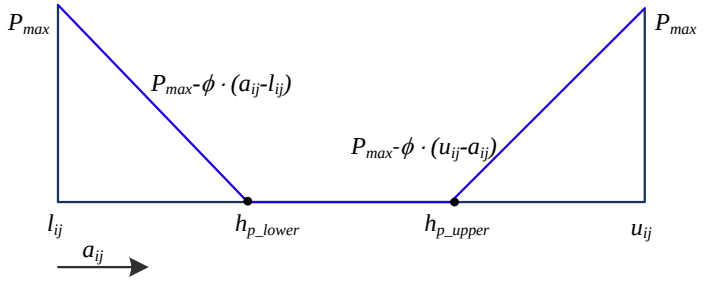

Figure 5: The designed penalty function curve

As an example, let us assume two headway activities with lower and upper bounds (l_{ij}, u_{ij}) equal to (2, 58) and (3, 57) respectively. For the first activity, we have $h_{ij}^{p\_lower} = 2 + (10 - 2) = 10$ min and $h_{ij}^{p\_upper} = 58 - (10 - 2) = 50$ min. For the second activity, we have $h_{ij}^{p\_lower} = 3 + (10 - 2) = 11$ min and $h_{ij}^{p\_upper} = 57 - (10 - 2) = 49$ min. Therefore, if the scheduled headway $a_{ij} = 4$, then the penalty becomes $\delta_{ij} = 80 - 10 \cdot (4 - 2) = 60$ in the first activity and $\delta_{ij} = 80 - 10 \cdot (4 - 3) = 70$ in the second activity. It could be found that the penalty value δ_{ij} is calculated according to the buffer times instead of the headway times, which is more reasonable in the railway timetable design.

Then the periodic timetabling model with timetable vulnerability *PESP-Vnb* is defined as:

$$\text{Minimize} \sum_{(i,j)\in A_{\text{head}}} \delta_{ij} \tag{18}$$

subject to (3)-(8) and

$$\delta_{ij} = w'_{ij} \cdot (P_{max} - \phi \cdot (a_{ij} - l_{ij})) + w'''_{ij} \cdot (P_{max} - \phi \cdot (u_{ij} - a_{ij})) \qquad \forall (i,j) \in \mathcal{A}_{\text{head}} \tag{19}$$

$$w'_{ij} + w''_{ij} + w'''_{ij} = 1 \qquad \forall (i,j) \in \mathcal{A}_{\text{head}} \tag{20}$$

$$w'_{ij}, w''_{ij}, w'''_{ij} \in \{0, 1\} \qquad \forall (i,j) \in \mathcal{A}_{\text{head}} \tag{21}$$

$$l_{ij} \le a_{ij} \le h_{ij}^{p\_lower} + M_1 \cdot (1 - w'_{ij}) \qquad \forall (i,j) \in \mathcal{A}_{\text{head}} \tag{22}$$

$$w''_{ij} \cdot h_{ij}^{p\_lower} < a_{ij} \le h_{ij}^{p\_upper} + M_2 \cdot (1 - w''_{ij}) \qquad \forall (i,j) \in \mathcal{A}_{\text{head}} \tag{23}$$

$$w'''_{ij} \cdot h_{ij}^{p\_upper} < a_{ij} \le u_{ij} \qquad \forall (i,j) \in \mathcal{A}_{\text{head}} \tag{24}$$

The penalty δ_{ij} for a headway activity is expressed as (19), which is a linearized version of (15). To model the piecewise function, three binary variables w'_{ij}, w''_{ij} and w'''_{ij} corresponding to each piece in (15) are introduced, and the big M method is used to construct the constraints. To be specific, the penalty δ contains three pieces of penalty value for each headway activity: (i) $w'_{ij}(P_{max} - \phi \cdot (a_{ij} - l_{ij}))$; (ii) $w''_{ij} \cdot 0$; (iii) $w'''_{ij}(P_{max} - \phi \cdot (u_{ij} - a_{ij}))$. The sum of binary variables is restricted to one in constraint (20), such that only one piece from the piecewise function could be counted in. Constraint (21) describes that w'_{ij}, w''_{ij} and w'''_{ij} are all binary variables. Constraints (22)-(24) guarantee that the value of a_{ij} is in the corresponding range if any of w'_{ij}, w''_{ij} and w'''_{ij} is 1. Big M_1 and M_2 can be selected as $u_{ij} - h_{ij}^{p\_lower}$ and $u_{ij} - h_{ij}^{p\_upper}$ respectively. The formulation of (19)-(24) is a general method to address a piecewise continuous function. For the special case of this minimization problem, the piecewise linear convex function (15) could also be expressed by three inequality constraints without binary variables which improves the computational efficiency. For the computational results in this paper, we used the general formulation.

2.2.4. *Flexible overtaking model (PESP-Ovt)*

We design our flexible overtaking to allow multiple overtakings of a stopped train based on Zhang and Nie (2016), and cover all different overtaking types as shown in Figure 6. Zhang and Nie (2016) introduced constraints for one passing train overtaking a stopped train (Figure 6 (a)), and proved that the overtaking occurs only if the sum of four modulo parameters of related dwell and headway activity equals 1 or 3, while 0 or 2 means no overtaking occurs (explanations are similar to the illegal overtaking in Section 2.2.1). For railway lines with mixed traffic of passenger and freight trains, multiple overtakings could be more useful as freight trains have a lower speed and little stops, and are less sensitive to dwell time loss. Hence, we extend the constraints to multiple overtakings in our flexible overtaking model. Section 4.3 compares the new model with multiple overtakings and the single overtaking constraints in Zhang and Nie (2016), which shows the benefit of this extension. Not only robustness and capacity, but also train journey time and regularity benefit from our flexible overtaking model.

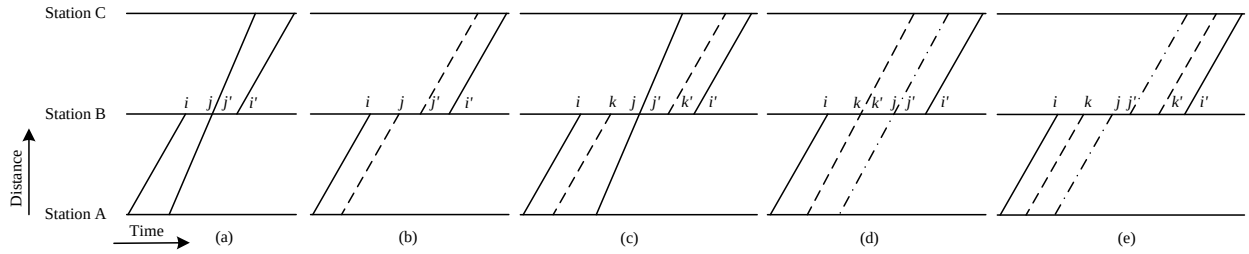

Figure 6: Five representatives of overtakings

A new binary variable $p_{ii'jj'}$ is proposed to indicate the existence of overtaking between activities (i, i') and (j, j'). If yes, it equals 1, and 0 otherwise. We restrict here (i, i') to be a dwell activity, so (j, j') can be either a dwell or through activity. In addition, binary variable $y_{ii'jj'}$ is introduced to represent the overtaking train order. It is 1 if activity (j, j') overtakes (i, i'), and 0 otherwise. For instance, in Figure 6 (a), overtaking occurs between activity (i, i') and (j, j'), so $p_{ii'jj'} = 1$ and $p_{jj'ii'} = 1$; activity (i, i') is overtaken by activity (j, j'), so $y_{ii'jj'} = 1$ and $y_{jj'ii'} = 0$. Variable $o_{ii'jj'}$ is an auxiliary binary variable, ensuring that the sum of modulo parameters is between 0 and 3 together with $p_{ii'jj'}$. Figure 7 illustrates the relationships of modulo parameters z_{ij}, $z_{i'j'}$, $z_{ii'}$ and $z_{jj'}$, and corresponding values of binary variable $p_{ii'jj'}$, $y_{ii'jj'}$ and $y_{jj'ii'}$ when the overtaking occurs at station B with overtaking type of Figure 6 (b). Note that all these related activities should be from the same station. Hence we also define $\mathcal{A}^{s_k}_{\text{dwell}}$, $\mathcal{A}^{s_k}_{\text{thru}}$, and $\mathcal{A}^{s_k}_{\text{head}}$ to represent dwell activities, through activities and headway activities at station s_k respectively.

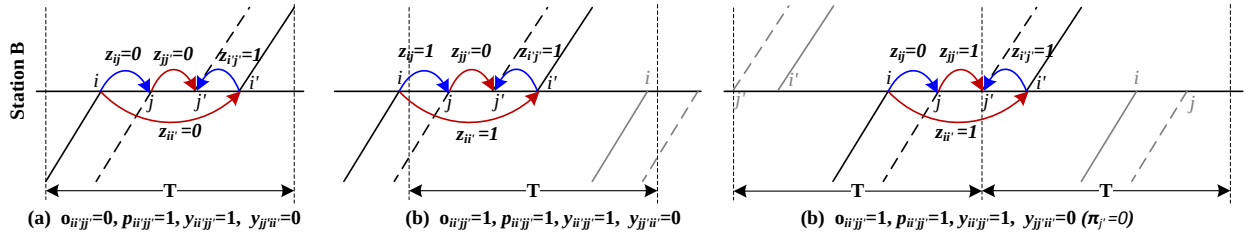

Figure 7: Three relationships between modulo parameters, and the corresponding values of binary variables $o_{ii'jj'}$, $p_{ii'jj'}$, $y_{ii'jj'}$ and $y_{jj'ii'}$ when an overtaking occurs at station B. Note: the red line represents the dwell activity, and the blue line for the headway activity

During the optimization process, in order to control the train with the minimum dwell time when no overtaking occurs, and limit the dwell time extension, a parameter h_{s_k} is designed as the maximum headway time at station s_k:

$$h_{s_k} = \max_{(i,j)\in\mathcal{A}^{s_k}_{\text{head}}} \{l_{ij}, T - u_{ij}\}$$

In addition, a parameter $d_{jj'}$ is defined as the maximal (dwell) time supplements for activity (j, j'),

$$d_{jj'} = u_{jj'} - l_{jj'}$$

If (j, j') is a through activity, $u_{jj'} = l_{jj'} = 0$ and thus also $d_{jj'} = 0$. We assume that the minimum dwell time at one station for all train lines are the same. If overtaking is allowed at the corresponding station, the dwell time supplement $d_{jj'}$ should become larger than $l_{ij} + l_{i'j'}$. In order to incorporate station capacity, a parameter $O^{max}_{s_k}$ is introduced as the maximum overtaking capacity at station s_k, i.e., the maximum number of siding tracks in station s_k. Finally, a binary variable $x_{ii'}$ is introduced to present whether dwell activity (i, i') is overtaken by through activities. If a passing overtaking exists at dwell activity (i, i'), it is 1, and 0 otherwise.

In general, an overtaking implies a longer dwell time, thus it is a disadvantage to the passengers in the train that waits to be overtaken by another train. Moreover, the tight headways between two overtaking trains also make the timetable more vulnerable. On the other side, overtakings could help to decrease capacity utilization when a faster train can overtake a slow train, which can then be used to run more trains, have more buffer between trains (elsewhere), or even enable to schedule the total number of trains in the first place. So the total number of overtakings are introduced to be optimized, and the trade-offs between overtakings and robustness/capacity are main timetabling design decisions. Hence, the periodic timetabling model with flexible overtaking *PESP-Ovt* is expressed as:

$$\text{Minimize} \sum_{s_k \in \mathcal{S}} \sum_{(i,i') \in \mathcal{A}^{s_k}_{\text{dwell}}} \sum_{(j,j') \in \mathcal{A}^{s_k}_{\text{dwell}} \cup \mathcal{A}^{s_k}_{\text{thru}}} y_{ii'jj'} \tag{25}$$

subject to (3)-(8) and

$$z_{ij} + z_{i'j'} + z_{ii'} + z_{jj'} = 2 \cdot o_{ii'jj'} + p_{ii'jj'} \quad \forall (i,i') \in \mathcal{A}^{s_k}_{\text{dwell}}, (j,j') \in \mathcal{A}^{s_k}_{\text{dwell}} \cup \mathcal{A}^{s_k}_{\text{thru}}, (i,j), (i',j') \in \mathcal{A}^{s_k}_{\text{head}}, s_k \in \mathcal{S} \tag{26}$$

$$y_{ii'jj'} + y_{jj'ii'} = p_{ii'jj'} \quad \forall (i,i') \in \mathcal{A}^{s_k}_{\text{dwell}}, (j,j') \in \mathcal{A}^{s_k}_{\text{dwell}} \cup \mathcal{A}^{s_k}_{\text{thru}}, (i,j), (i',j') \in \mathcal{A}^{s_k}_{\text{head}}, s_k \in \mathcal{S} \tag{27}$$

$$o_{ii'jj'}, p_{ii'jj'}, y_{ii'jj'}, y_{jj'ii'} \in \{0,1\} \quad \forall (i,i') \in \mathcal{A}^{s_k}_{\text{dwell}}, (j,j') \in \mathcal{A}^{s_k}_{\text{dwell}} \cup \mathcal{A}^{s_k}_{\text{thru}}, (i,j), (i',j') \in \mathcal{A}^{s_k}_{\text{head}}, s_k \in \mathcal{S} \tag{28}$$

$$-y_{jj'ii'} \cdot d_{jj'} - (1 - p_{ii'jj'}) \cdot (u_{jj'} - l_{ii'}) \leq a_{ii'} - a_{jj'} \leq y_{ii'jj'} \cdot d_{ii'} + (1 - p_{ii'jj'}) \cdot (u_{ii'} - l_{jj'}) \quad \forall (i,i') \in \mathcal{A}^{s_k}_{\text{dwell}}, (j,j') \in \mathcal{A}^{s_k}_{\text{dwell}} \cup \mathcal{A}^{s_k}_{\text{thru}}, s_k \in \mathcal{S} \tag{29}$$

$$x_{ii'} \in \{0,1\} \quad \forall (i,i') \in \mathcal{A}_{\text{dwell}} \tag{30}$$

$$\frac{1}{M} \sum_{(j,j') \in \mathcal{A}^{s_k}_{\text{thru}}} y_{ii'jj'} \leq x_{ii'} \leq \sum_{(j,j') \in \mathcal{A}^{s_k}_{\text{thru}}} y_{ii'jj'} \quad \forall (i,i') \in \mathcal{A}^{s_k}_{\text{dwell}}, s_k \in \mathcal{S} \tag{31}$$

$$a_{ii'} \leq l_{ii'} + 2 \cdot h_{s_k} \cdot \left(\sum_{(j,j') \in \mathcal{A}^{s_k}_{\text{dwell}}} y_{ii'jj'} \right) + h_{s_k} \cdot \left(\sum_{(j,j') \in \mathcal{A}^{s_k}_{\text{thru}}} y_{ii'jj'} \right) + x_{ii'} \cdot (h_{s_k} - l_{ii'}) \quad \forall (i,i') \in \mathcal{A}^{s_k}_{\text{dwell}}, s_k \in \mathcal{S} \tag{32}$$

$$\sum_{(i,i') \in \mathcal{A}^{s_k}_{\text{dwell}}} p_{ii'jj'} \leq O^{max}_{s_k} \quad \forall (j,j') \in \mathcal{A}^{s_k}_{\text{dwell}} \cup \mathcal{A}^{s_k}_{\text{thru}}, s_k \in \mathcal{S} \tag{33}$$

Constraints (26)-(29) formulate the relationships of activities from two different trains for flexible overtaking at a station. Constraint (26) describes that the sum of four modulo parameters is between 0 and 3. Variable $p_{ii'jj'}$ is 1 if an overtaking occurs, and 0 otherwise. The value of auxiliary variable $o_{ii'jj'}$ does not affect the occurrence of overtakings. Constraint (27) guarantees that at most one overtaking occurs between activity (i, i') and (j, j'). If $p_{ii'jj'}$ is 0, no overtaking exists. If $p_{ii'jj'}$ is 1, the overtaking could only occur once even if both are dwell activities, i.e., $y_{ii'jj'}$ or $y_{ii'jj'}$ equals 1. Moreover, constraint (29) is applied to obtain the values of variables $y_{ii'jj'}$ and $y_{ii'jj'}$ by restricting the relationship between both activities. In addition, certain overtakings can be fixed if needed by predefining the related variables and relationships between modulo parameters. Constraints (30)-(33) represent the restrictions of activity time and station capacity for multiple overtakings at one stop. Constraint (30) describes the binary variable for the existence of passing overtakings, and constraint (31) linearizes it by the total number of passing overtakings. Big M is a large number, which can be set as the maximal number of overtakings of all stations $\max_{s_k \in \mathcal{S}} O^{max}_{s_k}$. If the number of passing overtakings equals 0, then the upper bound ensures $x_{ii'}$ to be 0. Otherwise, if the number of passing overtakings is bigger than 0, the lower bound guarantees it to be 1. Constraint (32) allows extending dwell time only

when the overtaking happens and limits it depending on the number of passing overtakings and stopping overtakings. Constraint (33) guarantees that the number of overtakings at each station is no more than the overtaking capacity, which also can be used for dealing with platform capacity.

Dwell time extensions for different overtaking types are considered in constraint (32). To be specific, take overtaking examples from Figure 6. We assume 2 overtaking tracks available at station B with a minimum dwell time 1 min, and the minimum headway time is 3 min except for arrival-through and through-departure with 2 min. Table 1 shows the total number of overtakings between two dwell activities, the total number of overtakings between dwell and through activities, the existence of through overtaking, the minimal dwell time extension, and the computed maximal dwell time extension. For example, the maximal dwell time extension of Figure 6 (a) is computed as $l_{ii'} + 2 \cdot h_{s_k} \cdot 0 + h_{s_k} \cdot 1 + 1 \cdot (h_{s_k} - l_{ii'}) = 2 \cdot h_{s_k} = 6$. This is the input constraint to restrict the dwell time extension to be 0 when no overtaking occur, and to vary in a limited range when overtaking occurs.

Table 1: Values of parameters and variables for different overtaking types

Instance	$\sum_{(j,j')\in\mathcal{A}_{\text{dwell}}} y_{ii'jj'}$	$\sum_{(j,j')\in\mathcal{A}_{\text{thru}}} y_{ii'jj'}$	$x_{ii'}$	$a_{ii'}^{min}$	$a_{ii'}^{max}$
Figure 6 (a)	0	1	1	4	6
Figure 6 (b)	1	0	0	7	7
Figure 6 (c)	1	1	1	10	12
Figure 6 (d)	0	2	1	9	9
Figure 6 (e)	2	0	0	13	13
No overtaking	0	0	0	1	1

2.2.5. MOPRT

In section 2.2, four timetabling models with a single-objective were formulated. In order to find an optimal solution with consideration of all objectives above, a multi-objective periodic railway timetabling model including train journey time Z_{TJT}, timetable regularity deviation Z_{Reg}, timetable vulnerability Z_{Vnb} and the number of overtakings Z_{Ovt} as objectives to be minimized is proposed as follows:

$$Z_{TJT} = \sum_{(i,j)\in\mathcal{A}_{\text{run}}\cup\mathcal{A}_{\text{dwell}}} \alpha_{ij} \cdot (\pi_j - \pi_i + z_{ij} \cdot T) \tag{34}$$

$$Z_{Reg} = \sum_{(i,j)\in A_{\text{reg}}} \theta_{ij} \tag{35}$$

$$Z_{Vnb} = \sum_{(i,j)\in A_{\text{head}}} \delta_{ij} \tag{36}$$

$$Z_{Ovt} = \sum_{(i,j)\in A_{\text{dwell}}} y_{ii'jj'} \tag{37}$$

subject to (3)-(8), (11)-(12), (19)-(21), (26)-(33).

3. Pareto frontier

Multi-objective optimization aims to explore the Pareto (non-dominated) optimal solution set or quantify the trade-offs in fulfilling the different objectives. Marler and Arora (2004) investigated many approaches for multi-objective optimization for engineering, including the weighted sum method, ε-constraint method, normal boundary intersection method, and genetic (evolutionary) algorithms. Mavrotas (2009) mentioned that the ε-constraint method has four main advantages over the weighted sum, and Mavrotas and Florios (2013) developed an effective implementation of the ε-constraint method for generating the Pareto-optimal solutions with multi-objectives by comparing it with some meta-heuristic methods. Recently, the ε-constraint method was applied to solve railway multi-objective optimization problems for rescheduling with three objectives and capacity analysis with two objectives in Binder et al. (2017) and Burdett (2015), respectively. It was proved to be efficient for trade-off analysis, as well as yielding the Pareto optimal

solutions. Hence, the ε-constraint method is adopted to address our MOPRT problem. In the ε-constraint method, the multi-objective problem is optimized with one chosen objective function using the other objective functions as constraints. Different values of ε are used as the bound on the other functions. Solving the model by varying ε-constraint bounds, the Pareto frontier can be obtained.

To construct the Pareto frontier for the MOPRT from Section 2.2.5, four objectives (train journey times, timetable regularity, timetable vulnerability and the number of overtakings) need to be optimized in a priority order. Both passengers and train operators give the highest priority to total train journey time, as it is the fundamental factor for passengers travel choice and transport efficiency. So we put it in the first place to optimize. Regularity is the main idea of periodic timetabling, and vulnerability is used to improve timetable robustness by reducing the impact of delays. More overtakings could increase the train journey times, but at the same time decrease network capacity utilization and add more buffer times especially for a dense corridor. A regular scheduled timetable is convenient and attracts more passengers (Wardman et al., 2004), whereas robustness is useful when delays occur and overtakings could have a significant effect on both robustness and regularity when the railway capacity is tight at the cost of increased travel times. Thus at the planning level, we optimize regularity secondly, to preserve it as much as possible, followed by the vulnerability, and last overtaking.

Therefore, the following order is formulated to explore the Pareto frontier. Firstly, Z_{TJT} is computed, secondly Z_{Reg} with an upper bound on Z_{TJT}, thirdly Z_{Vnb} with upper bounds on both Z_{Reg} and Z_{TJT}, and finally Z_{Ovt} with upper bounds on all the other objectives. The upper bounds ε corresponding to each objective are denoted as ε_{TJT}, ε_{Reg}, ε_{Vnb} and ε_{Ovt}.

Moreover, the range of each objective function needs to be identified for providing effective values of ε-constraints. Traditionally, a payoff table, including ranges of objective values, could be obtained by solving each optimization problem with the corresponding single objective individually. When doing so, values of upper bounds tend to be arbitrary, and they could not ensure that the optimized solutions are Pareto optimal (Mavrotas, 2009), as an alternative optimal solution sometimes exists outside the given. Alternatively, too big values of upper bounds make the problem inefficient to solve. Therefore, we introduce Algorithm 1 with an adaptive payoff method to narrow the objective ranges in Section 3.1, especially to get effective computations with limited grids for the following steps. Moreover, with the given ε-constraints, infeasibility could occur in our minimization models (PESP-Vnb and PESP-Ovt) due to conflicts between constraints. To this end, Algorithm 2 is designed for a feasibility exploration in Section 3.2, to reduce the unnecessary computations for calculating solutions of Pareto-optimal set. Finally, Section 3.3 presents the Algorithm 3 for generating the Pareto frontier.

3.1. Compute adaptive payoff table

We propose an adaptive method to generate the payoff table and the Pareto frontier. An example of a payoff table is displayed in Table 2. The values in this table are obtained by solving each single-objective models independently, with1, 2, 3 and 4 representing each single-objective optimization model by the proposed priority order. To be more concrete, we use Table 4 from the later case study as an example. The values in each row are computed from the optimal solution of the corresponding single-objective model in the first column. For example, the values (27006, 12132, 64460, and 7) in the second row of Table 4 are computed from the PESP-TJT. The diagonal values (27006, 4692, 3912 and 7) are the optimal values from the models of PESP-TJT, PESP-Reg, PESP-Vnb and PESP-Ovt respectively, indicated as Z^{min}_{TJT}, Z^{min}_{Reg}, Z^{min}_{Vnb} and Z^{min}_{Ovt}. The initial maximal value for each objective is $Z^{max}_{TJT} = \max(Z_{TJT}(1), Z_{TJT}(2), Z_{TJT}(3), Z_{TJT}(4)) = \max(27006, 38112, 37634, 30654) = 38112$, and likewise for Z^{max}_{Reg} and Z^{max}_{Vnb}. Z^{max}_{Ovt} is not necessary to compute as PESP-Ovt is the last model to optimize. The process of updating upper bounds needs to be done one by one, and following the priority order: Z_{TJT}, Z_{Reg}, and Z_{Vnb}. It is the same for all objectives, except for the different numbers of iterations. Algorithm 1 presents this process for Z_{TJT}, while the other two objectives are treated in the same way. First, we find row i such that $Z_{TJT}(i) = Z^{max}_{TJT}$ and solve PESP-TJT by adding constraints $Z_{Reg} \leq Z_{Reg}(i)$, $Z_{Vnb} \leq Z_{Vnb}(i)$, and $Z_{Ovt} \leq Z_{Ovt}(i)$, i.e., $Z_{TJT}(2) = 38112$ and added constraints $Z_{Reg} \leq 4692$, $Z_{Vnb} \leq 58820$, and $Z_{Ovt} \leq 12$. Then the new optimized value Z_{TJT} is updated in row i of the payoff table, as well as Z_{Reg}, Z_{Vnb}, and Z_{Ovt}, which are calculated from the solution of this optimization. Moreover, we recompute the maximal objective value $Z^{max}_{TJT} = \max(Z_{TJT}(1), Z_{TJT}(2), Z_{TJT}(3), Z_{TJT}(4))$ in this updated payoff table. If $Z^{max}_{TJT} = Z_{TJT}(i)$, the objective value could no longer be improved under the constraints of the other objectives. This value would be selected as the upper bound of Z_{TJT}. If $Z^{max}_{TJT} > Z_{TJT}(i)$, we repeat all previous steps until $Z_{TJT}(i) = Z^{max}_{TJT}$, with the generated upper bound.

Table 2: Payoff table obtained by solving single-objective models

Models	Z_{TJT}	Z_{Reg}	Z_{Vnb}	Z_{Ovt}
PESP-TJT	$Z_{TJT}(1)$	$Z_{Reg}(1)$	$Z_{Vnb}(1)$	$Z_{Ovt}(1)$
PESP-Reg	$Z_{TJT}(2)$	$Z_{Reg}(2)$	$Z_{Vnb}(2)$	$Z_{Ovt}(2)$
PESP-Vnb	$Z_{TJT}(3)$	$Z_{Reg}(3)$	$Z_{Vnb}(3)$	$Z_{Ovt}(3)$
PESP-Ovt	$Z_{TJT}(4)$	$Z_{Reg}(4)$	$Z_{Vnb}(4)$	$Z_{Ovt}(4)$

Algorithm 1: Updating payoff table for objective Z_{TJT}

Input: Line plan, timetable related parameters, payoff table
Output: Updated payoff table
Generate the event-activity network
repeat
  Find row i with $Z_{TJT}(i) = \max(Z_{TJT}(1), Z_{TJT}(2), Z_{TJT}(3), Z_{TJT}(4))$ in the payoff table
  Solve PESP-TJT with extra constraints $Z_{Reg} \leq Z_{Reg}(i)$, $Z_{Vnb} \leq Z_{Vnb}(i)$, and $Z_{Ovt} \leq Z_{Ovt}(i)$
  Update new optimized values of Z_{TJT}, Z_{Reg}, Z_{Vnb} and Z_{Ovt} in row i of the payoff table
  Set $Z^{max}_{TJT} = \max(Z_{TJT}(1), Z_{TJT}(2), Z_{TJT}(3), Z_{TJT}(4))$ from this updated payoff table
until $Z_{TJT}(i) = Z^{max}_{TJT}$

With the updated upper bound values in the payoff table, the ranges of Z_{TJT}, Z_{Reg}, and Z_{Vnb} are known. We then divide each range into equal intervals by a proposed number of grid points for computing Pareto solutions. Here, N_{TJT}, N_{Reg} and N_{Vnb} represent the number of grid points of each objective. The more points, the finer the found Pareto frontier but at the same time more iterations are needed for solving the problem. The value set of ε-constraints for the TJT objective function is

$$C^n_{TJT} = Z^{min}_{TJT} + (n-1) \cdot \frac{Z^{max}_{TJT} - Z^{min}_{TJT}}{N_{TJT}} \quad n = 1, ..., N_{TJT}.$$

Set C_{TJT} represents the constraint value set, defined as $C_{TJT} = \{C^1_{TJT}, ..., C^{N_{TJT}}_{TJT}\}$. Sets C_{Reg} and C_{Vnb} are defined in the same way.

3.2. Explore the model feasibility

When the value sets for the ε-constraints have been determined, the computation to explore the Pareto frontier for the MOPRT model can be conducted. However, we observed that PESP-Ovt could be infeasible with some combinations of constraints ε_{TJT}, ε_{Reg} and ε_{Vnb}. The reason may be that at least two objective values have comparable small upper bounds of ε-constraints, which are not possible to achieve in one solution. This issue could already exist in three dimensions for the multi-objective model: PESP-TJT, PESP-Reg, and PESP-Vnb. Hence, we introduce a feasibility check in the three-dimension variant to remove the combinations of infeasible ε-constraints, which could help to improve the computation efficiency in our MOPRT model.

Algorithm 2 explains the process to check the feasibility of PESP-Vnb with two extra ε-constraints: C_{TJT} and C_{Reg}. With the given input of line plan and timetable related data (running times, dwell time, headway times, etc.), the event-activity network is generated first.

We initialize Ω and $\mathcal{R}$ as two empty sets. The former is to store n and r combinations of ε-constraints from feasible solutions, and the latter is to save the obtained solutions indexed by m. We set the ε-constraint values of C_{TJT} and C_{Reg} varying from the most relaxed to the most restrictive ones. For each n, we vary r from N_{Reg} to 0, and repeat solving PESP-Vnb with new extra constraints of $Z_{TJT} \leq C^n_{TJT}$ and $Z_{Reg} \leq C^r_{Reg}$, save the pair (n, r) in Ω and the current objective results in $\mathcal{R}$ until the solution is infeasible or $r = 0$. If it is infeasible or $r = 0$, then n is reduced by 1 and we repeat the previous steps until $n = 0$. In this way, for a certain n, if PESP-Vnb is infeasible for $\varepsilon_{Reg} = C^r_{Reg}$, the following iterations $r - 1, ..., 1$ could be skipped because these iterations will also lead to infeasibility.

Algorithm 2: Explore the feasibility space of model PESP-Vnb with ε-constraints ε_{TJT} and ε_{Reg}

Input: Line plan, timetable related parameters, C_{TJT}, and C_{Reg}
Output: Feasbile constraint index set Ω

Initialization $\Omega \leftarrow \emptyset$, feasible solution set $\mathcal{R} \leftarrow \emptyset$, feasible solution index $m \leftarrow 1$
Generate the event-activity network
for $n = N_{TJT}$ **to** 1 **do**
  $\varepsilon_{TJT} \leftarrow C^n_{TJT}$
  $r \leftarrow N_{Reg}$
  repeat
    $\varepsilon_{Reg} \leftarrow C^r_{Reg}$
    Solve PESP-Vnb with extra constraints $Z_{TJT} \leq \varepsilon_{TJT}$ and $Z_{Reg} \leq \varepsilon_{Reg}$
    $\Omega \leftarrow \{n, r\}$
    Calculate objective values of Z^m_{TJT} and Z^m_{Reg}
    Save current solution in $\mathcal{R}$
    $m \leftarrow m + 1$
    $r \leftarrow r - 1$
  until $r = 0$ **or** *Model PESP-Vnb is infeasible*

Only pairs of n and r in Ω need to be calculated when solving MOPRT with four objectives as feasibility cannot be restored. If a model could not be solved, then it is also infeasible when more restrictive constraints and/or different objectives are added.

3.3. Generate Pareto-optimal solutions

In multi-objective optimization, when the different objectives are contradictory, an optimal solution is considered as the Pareto optimal when it is not possible to improve one objective without degrading the others. The set of all Pareto optimal solutions is called the Pareto frontier as it usually graphically forms a distinct front of points. Solutions which do not lay on the Pareto front are called Pareto dominated solutions. Hence, Algorithm 3 is designed to explore the Pareto frontier of the four-objective timetabling model under ε-constraints. We initialize Ψ and $\mathcal{X}$ as two empty sets. The former is to store all feasible solutions indexed by k, and the latter is to store the index of dominated solutions. For each pair (n, r) in Ω, the corresponding constraints $Z_{TJT} \leq C^n_{TJT}$, $Z_{Reg} \leq C^r_{Reg}$ are generated. Then the model PESP-Ovt is solved for each b with constraints $\varepsilon_{Vnb} = C^b_{Vnb}$ (b is varying from N_{Vnb} to 1) iteratively until an infeasible solution occurs or $b = 0$. If the model is feasible, each objective value Z^k_{TJT}, Z^k_{Reg} and Z^k_{Vnb} (k the index of the current solution) is also calculated, and saved in Ψ together with Z^k_{Ovt}. When all computations are done, we check the dominance of solutions in set Ψ to obtain the Pareto-optimal set. For a solution $\Psi(k)$, we check whether a better solution $\Psi(q)$ with smaller Z^q_{TJT}, Z^q_{Reg}, Z^q_{Vnb}, and Z^q_{Ovt} exists. If satisfying $Z^q_{TJT} \leq Z^k_{TJT}$, $Z^k_{Reg} \leq Z^k_{Reg}$, $Z^q_{Vnb} \leq Z^k_{Vnb}$, and $Z^q_{Ovt} \leq Z^k_{Ovt}$ (at least including one strict inequality of all four inequalities), this solution is removed from Ψ. Finally, a Pareto optimal solution set is achieved.

3.4. Normalization of objective values

When the Pareto optimal set is generated, rail operators could select the timetable according to their preference. However, it is still difficult to choose, and an overall optimal solution is still necessary to be discussed. To compare the difference between solutions, standardized Euclidean distance (distance to zero) is proposed. First, the values of each objective are normalized. For Z_{TJT}, a normalized objective function is:

$$\widetilde{Z}^k_{TJT} = \frac{Z^k_{TJT} - Z^{min}_{TJT}}{Z^{max}_{TJT} - Z^{min}_{TJT}}, \tag{38}$$

Algorithm 3: Explore the Pareto frontier of the MOPRT model under ε-constraints

Input: Line plan, timetable related parameters, C_{TJT}, C_{Reg}, C_{Vnb}, Ω
Output: Pareto frontier of the MOPRT model

Initialization: solution set $\Psi \leftarrow \emptyset$, solution index $k \leftarrow 1$, set of dominated solution index $\mathcal{X} \leftarrow \emptyset$
for $(n, r) \in \Omega$ **do**
  $\varepsilon_{TJT} \leftarrow C^n_{TJT}$
  $\varepsilon_{Reg} \leftarrow C^r_{Reg}$
  $b \leftarrow N_{Vnb}$
  repeat
    $\varepsilon_{Vnb} \leftarrow C^b_{Vnb}$
    Solve PESP-Ovt with extra constraints $Z_{TJT} \leq \varepsilon_{TJT}$, $Z_{Reg} \leq \varepsilon_{Reg}$ and $Z_{Vnb} \leq \varepsilon_{Vnb}$
    Calculate objective values of Z^k_{TJT}, Z^k_{Reg} and Z^k_{Vnb}
    Save current solution in Ψ
    $k \leftarrow k + 1$
    $b \leftarrow b - 1$
  until $b = 0$ **or** *Model PESP-Ovt is infeasible*
$N(\Psi) \leftarrow$the number of solutions in Ψ
for $k = 1$ **to** $N(\Psi)$ **do**
  for $q = 1$ **to** $N(\Psi)$ **do**
    if $Z^q_{TJT} \leq Z^k_{TJT}$, $Z^q_{Reg} \leq Z^k_{Reg}$, $Z^q_{Vnb} \leq Z^k_{Vnb}$, *and* $Z^q_{Ovt} \leq Z^k_{Ovt}$ *including one strict inequality* **then**
      $\mathcal{X} \leftarrow \mathcal{X} + \{k\}$
Update $\Psi = \Psi \backslash \Psi(\mathcal{X})$ by removing results of iteration numbers in set $\mathcal{X}$.

and $\widetilde{Z}^k_{Reg}$, $\widetilde{Z}^k_{Vnb}$, and $\widetilde{Z}^k_{Ovt}$ are normalized in the same way. Then the standardized Euclidean distance of the $k-th$ solution ρ_k can be calculated:

$$\rho_k = \sqrt{(\widetilde{Z}^k_{TJT})^2 + (\widetilde{Z}^k_{Reg})^2 + (\widetilde{Z}^k_{Vnb})^2 + (\widetilde{Z}^k_{Ovt})^2} \tag{39}$$

The best solution is adopted such that $\rho^* = \min_{k\in[1,N((\Psi)]}\rho_k$. With a predefined Δ that $\rho^* + \Delta \in [min_{k\in[1,N((\Psi)]}\rho_k, 1]$, the best solution set Υ can also be achieved such that $\Upsilon =_{k\in[1,N((\Psi)]} \{\rho_k < \rho^* + \Delta\}$.

3.5. Evaluation criterion of capacity utilization

When the standardized Euclidean distance of each solution is calculated, the values from the best solution set are sometimes quite close to each other. Therefore, capacity utilization is implemented as an extra evaluation criterion to help to make a decision.

The minimum cycle time λ (Goverde, 2007) is used to represent the timetable capacity utilization. When train orders, and running times have been determined, λ can easily be computed by compressing the headways between successive trains towards their default values as much as possible. Then the capacity utilization of the obtained timetable with period length T can be calculated by

$$C = \frac{\lambda}{T} \tag{40}$$

Note that this capacity utilization indicator mainly focuses on the buffer times at stations, and is generated for macroscopic timetables with default minimum headways, which differs from the capacity occupation in UIC (2013) that uses microscopically computed blocking times to derive the minimum headway times exactly.

4. Experiments and computational results

To demonstrate the applicability of our MOPRT model and the Pareto frontier approach we use two cases. First, a theoretical case is used in Section 4.1 to demonstrate the feasibility and validity of each single-objective model and

the designed algorithms for exploring the Pareto-optimal solutions. The final adopted payoff table is generated by using Algorithm 1. The trade-off between objectives is analyzed with the computational results from exploration of the Pareto frontier (Algorithm 2 and Algorithm 3). Second, a real-world case of a Dutch railway corridor is applied in Section 4.2. We test the efficiency of our model by comparing the obtained optimal solution with the existing timetable. The optimization models and algorithms are implemented using Matlab R2017b, and the Yalmip toolbox (Löfberg, 2004) with Gurobi version 8.0.0.

4.1. Theoretical case

The first case is a double-track corridor with five stations and dense heterogeneous traffic. It is served by three train lines with different stopping patterns and frequencies of 4, 2 and 3 respectively. Figure 8 displays the given network layout and line plan. We only consider trains from A to E. Overtakings are allowed for all trains and the maximal overtaking capacities for the stations B, C and D are set to 2. A certain amount of dwell time supplement is allowed in the optimization process to allow the occurrence of overtakings. Table 3 depicts the parameter values applied in our model. The period length is set to one hour (3600 s). For train journey time, the weights of running and dwell activities are 1 and 3 respectively. The maximum dwell time supplement is 600 s to allow at most two overtakings of a train at one stop. A maximum regularity deviation of 420s is used to control that train lines from the same line still follow a certain regular pattern. Without loss of generality, only the traffic in the direction from A to E is considered.

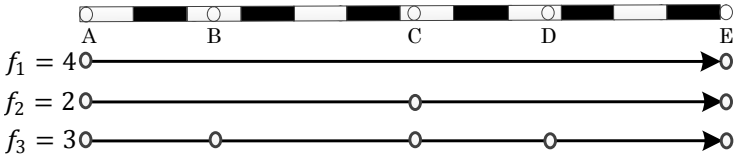

Figure 8: Line plan

Table 3: Input parameters of the MOPRT model

Parameter	Value
Period length T	3600 s
Weight of activity α_{ij}	1 if $(i, j) \in \mathcal{A}_{\text{run}}$, and 3 if $(i, j) \in \mathcal{A}_{\text{dwell}}$
Minimum dwell time l_{ij}	120 s $(i, j) \in \mathcal{A}_{\text{dwell}}$
Minimum headway time h_{ij}	180 s $(i, j) \in \mathcal{A}_{\text{head}}$
Maximum dwell time supplement d_{ij}	600 s $(i, j) \in \mathcal{A}_{\text{dwell}}$
Maximum regularity deviations β_l	420 s

4.1.1. Payoff table generation (using Algorithm 1)

By solving each single-objective optimization model independently, an initial payoff table including values of each objective is obtained, as shown in Table 4. Figure 9 illustrates the time-distance diagrams of the computed timetables from each single-objective model.

From Table 4, both timetables from PESP-TJT and PESP-Ovt (see Figure 9 (a) and Figure 9 (d)) have the the least number of overtakings (7 in total). However, it can be observed that the former has least dwell time supplement. Due to minimizing the deviations between departure and arrival intervals in PESP-Reg, it can be seen in Figure 9 (b) a strong regularity of trains from the same line, as well as similar dwell times at stations. Figure 9 (c) shows that headways between trains are always larger than the minimum headway except at stops compared with others, which demonstrates that PESP-Vnb could help to improve robustness. However, in order to achieve the optimal value of the corresponding objective, timetables from each of single-objective model have some drawbacks. Timetable from model PESP-TJT (Figure 9 (a)) has plenty of minimum headways and no regularity of trains. Both timetables from PESP-Reg (Figure 9 (b)) and PESP-Vnb (Figure 9 (c)) have lots of running time supplements and dwell time

Table 4: Initial payoff table obtained by each single-objective models

Model/objectives	Z_{TJT} [s]	Z_{Reg} [s]	Z_{Vnb} [s]	Z_{Ovt} [-]
PESP-TJT	27006	12132	64460	7
PESP-Reg	38112	4692	58820	12
PESP-Vnb	37634	17972	39120	12
PESP-Ovt	30654	13092	65500	7

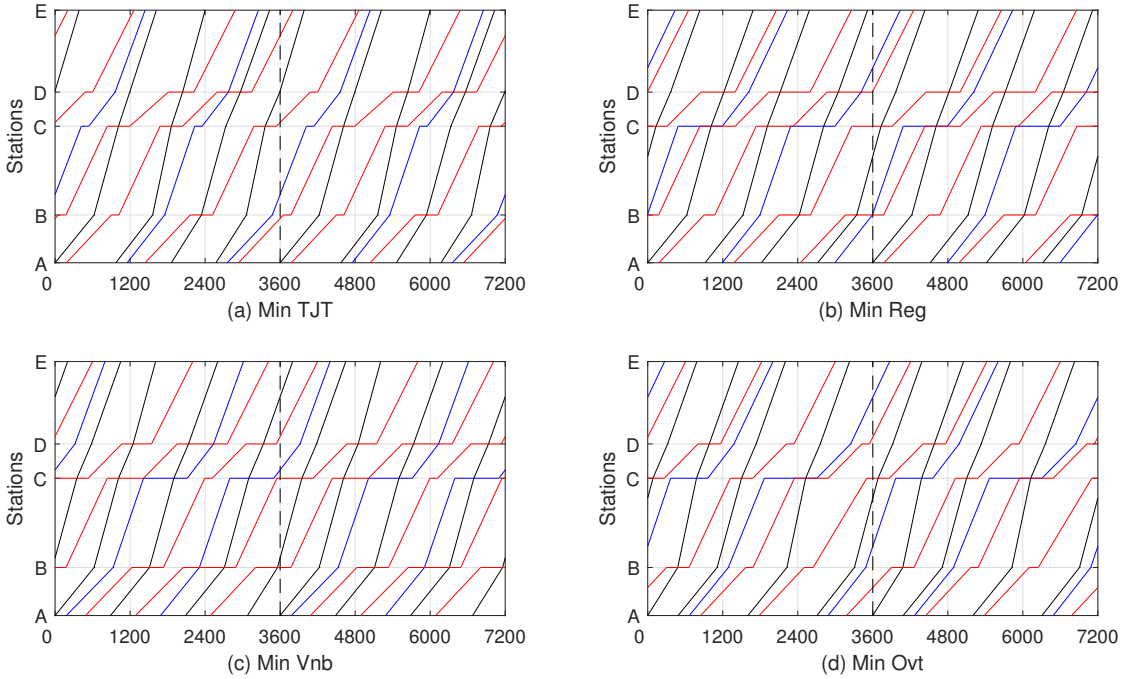

Figure 9: Time-distance diagrams of optimized timetable from (a) PESP-TJT, (b) PESP-Reg, (c) PESP-Vnb and (d) PESP-Ovt

supplements. Timetable from PESP-Ovt (Figure 9 (d)) has all the above-mentioned drawbacks. This also indicates that a single-objective is not enough to satisfy multiple requirements from rail operations and needs to be extended.

We update values in Table 4 to a more effective upper bound for each objective by Algorithm 1. Table 5 displays the updated payoff table, the explored range (including underlined minimal and maximal values of each objective). It can be found that the upper bound of Z_{TJT} and Z_{Vnb} decrease by 902 from 38112 to 37210, and 4190 from 65500 to 61310 respectively. To illustrate the exploration of the Pareto frontier without too much involved computations, 8 grid points are proposed for each of the three objectives Z_{TJT}, Z_{Reg}, and Z_{Vnb}.

Table 5: Updated payoff table (unit: s for objective Z_{TJT}, Z_{Reg}, and Z_{Vnb})

Models/Objectives	Z_{TJT}	Z_{Reg}	Z_{Vnb}	Z_{Ovt}
PESP-TJT	<u>27006</u>	12132	<u>61310</u>	7
PESP-Reg	36930	<u>4692</u>	58820	12
PESP-Vnb	<u>37210</u>	17972	<u>39120</u>	12
PESP-Ovt	30654	<u>13092</u>	46860	7

4.1.2. Feasibility exploration (using Algorithm 2)

This feasibility exploration could help to reduce the search space for the Pareto frontier of the MOPRT model. By conducting Algorithm 2, set Ω with combinations of feasible constraints is attained, giving 53 feasible solutions out of 64 possible solutions. As this algorithm is implemented at a three-dimension level with PESP-TJT, PESP-Reg, and PESP-Vnb, the trade-offs between these objectives could be analyzed in a clear way, especially to show how train journey time and timetable regularity impact the timetable vulnerability.

Figure 10 (a) shows the variation of train journey time (Z_{TJT}) and timetable vulnerability (Z_{Vnb}) for different regularity deviations (ε_{Reg}). It can be observed that the overall tendency is that smaller train journey times have a negative effect on timetable vulnerability, as expected. In detail, Z_{Vnb} becomes stable around 4.25×10^4 for Z_{TJT} varying between 3.28×10^4 and 3.58×10^4, and ε_{Reg} varying between 8486 and 16075 (data of the legend). Moreover, Z_{TJT} and Z_{Vnb} become quite insensitive when ε_{Reg} changes from 10383 to 17972. This reveals that ε_{Reg} has no noticeable impact on solutions when it becomes larger. Only when ε_{Reg} changes to the maximal value (17972), Z_{Vnb} could achieve its optimal value (39120) while Z_{TJT} is at its maximal value (37210). This indicates that the optimal solution with balanced objective values must occur above $Z_{Reg} = 10383$. Figure 10 (b) displays the relation between Z_{Reg} and Z_{Vnb} with different ε_{TJT}, showing that Z_{Vnb} decreases with increasing Z_{Reg} in general. However, the variation becomes quite small when Z_{Reg} raises to 10383, which agrees with Figure 10 (a). Meanwhile, the relation between Z_{Reg} and Z_{Vnb} is not much different for ε_{TJT} from 32837 to 37210, which is similar to the conclusion from Figure 10 (a). Most Z_{TJT} are around 32837 for this solution set. Therefore, if only the balanced optimal solution is needed, the constraint set Ω could be reduced by removing constraints of the captured values of $\varepsilon_{TJT} > 32873$ and $\varepsilon_{Reg} > 10383$. Nevertheless, in this paper, the whole set of Ω is required to generate different results to study the trade-offs between the objectives in the MOPRT model.

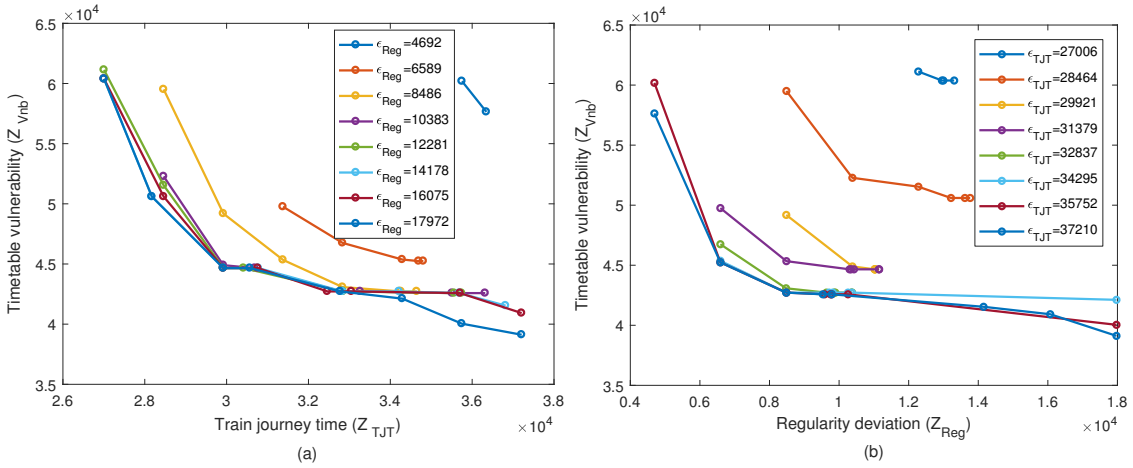

Figure 10: Trade-off between different objectives: (a) train journey time and timetable vulnerability for varying regularity deviation ε_{Reg}; (b) regularity devation and timetable vulnerability for varying train journey time ε_{TJT}

4.1.3. Pareto-optimal solutions generation (using Algorithm 3)

Algorithm 3 is designed for solving MOPRT model combining PESP-TJT, PESP-Reg, PESP-Vnb and PESP-Ovt and creating Pareto-optimal solutions. In total, 274 solutions are found while varying ε_{TJT}, ε_{Reg} and ε_{Vnb} within the given set Ω. Of that number, 83 non-dominated solutions are found generating the Pareto-optimal set. Figure 11 depicts these solutions by a 3D scatter plot with the color-bar representing the fourth objective of the number of overtakings. The top five solutions are quite nearby each other ($\Delta = 0.02$), see the red circle on the bottom (the best solution is shown with edge color red). In addition, the next three solutions 6-8 are also pointed out as comparable different objective values with the best solution ($\Delta = 0.1$).

According to the standardized Euclidean distance, Table 6 shows the best solution set Υ with $\Delta = 0.16$. For each solution, it includes the upper bounds of constraints (ε_{TJT}, ε_{Reg} and ε_{Vnb}), obtained objective values (Z_{TJT}, Z_{Reg},

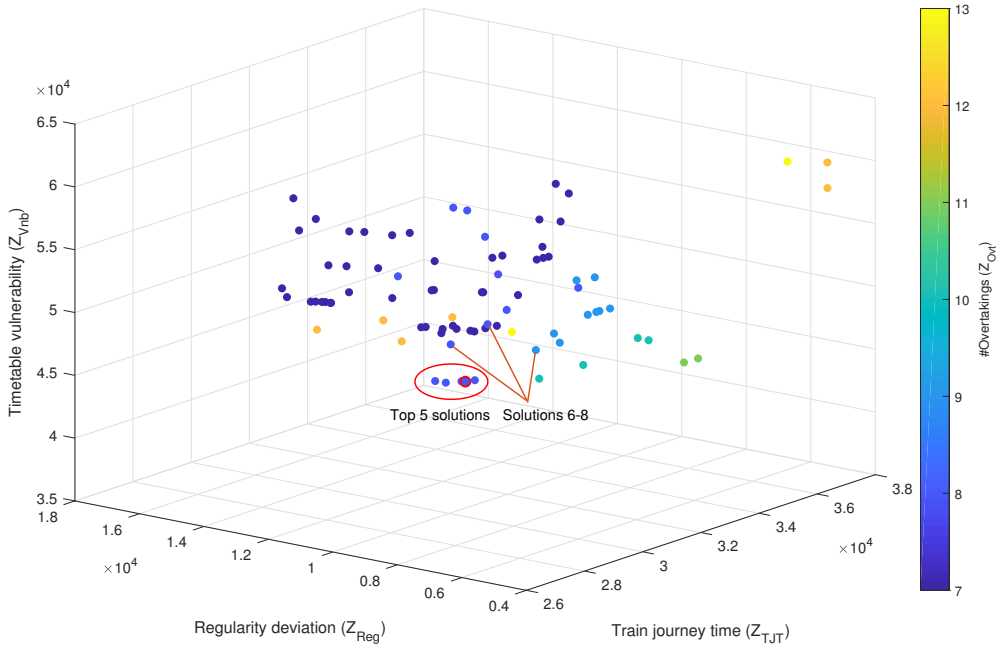

Figure 11: Pareto-optimal set

Z_{Vnb} and Z_{Ovt}), normalized objective values ($\widetilde{Z}_{TJT}$, $\widetilde{Z}_{Reg}$, $\widetilde{Z}_{Vnb}$ and $\widetilde{Z}_{Ovt}$), standardized Euclidean distance ρ, capacity utilization C, optimization gap and time. It can be observed that each Z_{Vnb} almost reaches its upper bound ε_{Vnb}, and so do most ε_{TJT} and ε_{Reg} with effective restrictions for the model. The objective values of timetable vulnerability have a bigger variation range than the other objectives observed from value range of $\widetilde{Z}_{TJT}$, $\widetilde{Z}_{Reg}$, $\widetilde{Z}_{Vnb}$, and $\widetilde{Z}_{Ovt}$. This means that timetable vulnerability has quite a remarkable impact to the final obtained solution. The number 0.0000 of $\widetilde{Z}_{Ovt}$ means that the optimized value of Z_{Ovt} has zero distance to the overall minimal value from Table 5.

Moreover, it can be observed that solutions with nine overtakings have lower capacity utilization than the others. This also can be verified by Figure 12, which depicts that the number of overtakings has an opposite effect on capacity utilization in the solutions from the Pareto-optimal set. However, there is no obvious difference between solutions with seven and eight overtakings. We select three best solutions with different number of overtakings to see the difference. The time-distance diagrams are plotted in Figure 13 for (a) the best solution No.1 with 8 overtakings per hour; (b) solution No.8 with 9 overtakings per hour; and (c) solution No.9 with 7 overtakings per hour. It can be observed that solution No.1 and solution No.9 almost have the same train orders except the existence of an overtaking between the train with the red line and blue line at station C. Instead of the overtaking in Figure 13(a), successive arrival and departure activities exist between two trains in Figure 13(c), which have the same strict infrastructure constraints as an overtaking. Therefore, the capacity utilization is similar in both solutions. In addition, it can be straightforwardly recognized that the timetables in Figure 13 are better than the ones in Figure 9 with a more reasonable allocation of time supplements and fewer overtakings. To contrast with the optimal objective values of the single-objective model, the best solution has 11.96%, 107.00%, 16.21% and 14.28% increase of Z_{TJT}, Z_{Reg}, Z_{Vnb} and Z_{Ovt}, respectively.

The 4D plot in Figure 11 is not adequate to analyze the trade-offs for all objectives as it is difficult to figure out the variation tendency. Therefore, we designed Figure 14 and Figure 15 with four subplots to illustrate the relations between all four objectives. Each subplot represents two dimensions directly and the third one roughly depicted by the face color of the circles. The darker the color, the higher the value (color-bar on the right side). From both figures, we can determine that train journey time Z_{TJT} has a positive effect on the number of overtakings Z_{Ovt}, and a negative effect on vulnerability Z_{Vnb} and regularity deviation Z_{Reg}. It can be clarified that overtakings lead to increasing the total dwell times, and more running time supplements are needed to pull trains as far as possible and keep trains operate regular. Overall, an increment of Z_{Vnb} could lead to a decrement of Z_{Ovt}, like more overtakings could help to improve robustness. No clear relations are derived between Z_{Reg} and Z_{Vnb}, Z_{Reg} and Z_{Ovt}, as the data in both subplots

Table 6: Partial Pareto-optimal solutions from the MOPRT model (sorted according to ρ)

No.	ε_{TJT} [s]	ε_{Reg} [s]	ε_{Vnb} [s]	Z_{TJT} [s]	Z_{Reg} [s]	Z_{Vnb} [s]	Z_{Ovt} [-]	$\widetilde{Z}_{TJT}$ [-]	$\widetilde{Z}_{Reg}$ [-]	$\widetilde{Z}_{Vnb}$ [-]	$\widetilde{Z}_{Ovt}$ [-]	ρ [-]	C [%]	gap [%]	Opt time [s]
1	35752	16075	45460	30236	9712	45460	8	0.3165	0.3780	0.2857	0.1667	0.5937	94.58	0.00	110.83
2	29921	12281	45460	29919	10032	45460	8	0.2855	0.4021	0.2857	0.1667	0.5938	95.19	0.00	121.35
3	37210	17972	45460	30225	9822	45440	8	0.3155	0.3863	0.2848	0.1667	0.5980	94.19	0.00	97.79
4	37210	10383	45460	30451	9612	45460	8	0.3376	0.3705	0.2857	0.1667	0.6005	94.17	0.00	68.30
5	29921	16075	45460	29888	10334	45460	8	0.2824	0.4248	0.2857	0.1667	0.6080	96.14	0.00	77.71
6	29921	10383	48630	29881	9846	48630	8	0.2818	0.3881	0.4286	0.1667	0.6644	95.61	0.00	115.76
7	29921	8486	51800	29642	8486	51110	8	0.2583	0.2857	0.5403	0.1667	0.6842	96.83	0.00	75.97
8	35752	8486	48630	30609	7862	48630	9	0.3531	0.2387	0.4286	0.3333	0.6902	92.69	0.00	1443.48
9	31379	10383	48630	31025	10144	48630	7	0.3939	0.4105	0.4286	0.0000	0.7123	95.06	0.00	47.57
10	37210	10383	48630	31023	10264	48630	7	0.3937	0.4196	0.4286	0.0000	0.7174	94.58	0.00	50.61
11	32837	10383	48630	31378	10118	48630	7	0.4285	0.4086	0.4286	0.0000	0.7309	94.56	0.00	44.36
12	32837	14178	48630	30972	10648	48620	7	0.3887	0.4485	0.4281	0.0000	0.7318	95.42	0.00	55.47
13	35752	8486	51800	30254	8446	51800	8	0.3183	0.2827	0.5714	0.1667	0.7318	95.50	0.00	87.40
14	32837	8486	48630	31396	7830	48630	9	0.4302	0.2363	0.4286	0.3333	0.7319	91.36	11.11	1814.24
15	35752	16075	48630	30779	10906	48630	7	0.3698	0.4679	0.4286	0.0000	0.7344	96.00	0.00	68.53
16	35752	10383	48630	31680	10038	48630	7	0.4581	0.4026	0.4286	0.0000	0.7453	94.00	0.00	60.97
17	32837	12281	48630	31120	11252	47860	7	0.4032	0.4940	0.3939	0.0000	0.7495	95.17	0.00	86.04
18	35752	12281	48630	30614	11422	48630	7	0.3536	0.5068	0.4286	0.0000	0.7520	94.89	0.00	60.61
19	34295	14178	48630	30693	11354	48630	7	0.3613	0.5017	0.4286	0.0000	0.7523	95.67	0.00	63.06

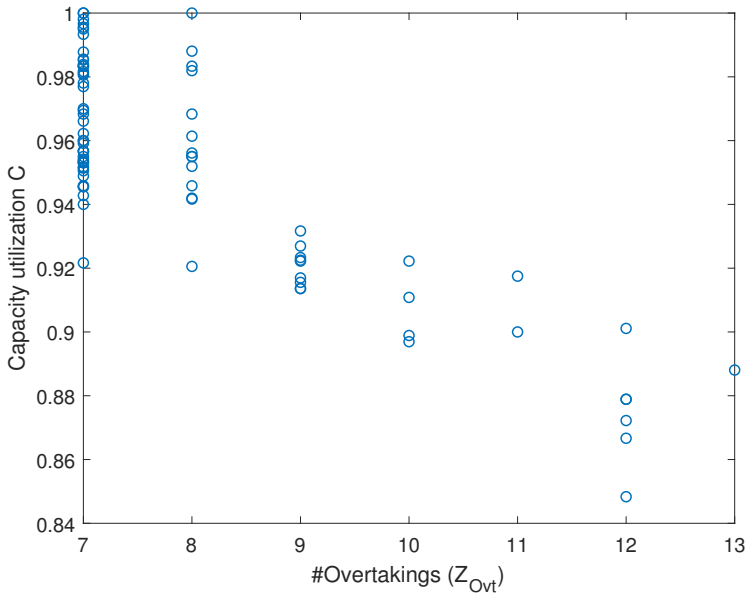

Figure 12: The relationship between the number of overtakings and capacity utilization

are scattered quite randomly. The circles connected by red dashed lines are the top five solutions, of which the one with the red edges is the best solution in both figures. In addition, the separated ones with the dark red edge are the top 6-8. Figure 15 also indicates some extreme results in the blue and purple dashed box. Solutions in the blue box are in the opposite direction of the variation tendency in the Z_{Reg} related subplots, and have quite large values for all Z_{TJT}, Z_{Reg} and Z_{Ovt}. The reason is that to reach the minimum timetable vulnerability, we need to have plenty of train journey time and regularity loss, and the number of overtakings increases to compensate for obtaining the best robust

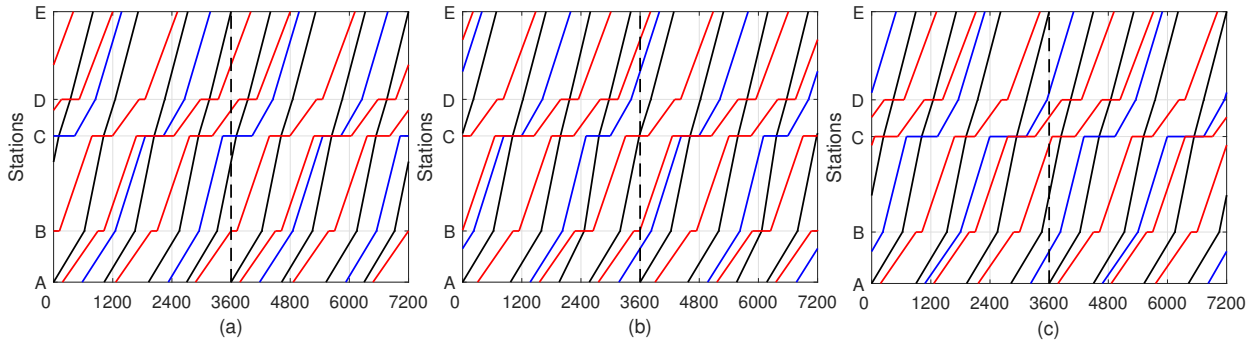

Figure 13: Time-distance diagrams of two periods: (a) The best solution No.1 with 8 overtakings per hour; (b) Solution No.8 with 9 overtakings per hour; (c) Solution No.9 with 7 overtakings per hour

timetable. Similarly, solutions in the purple box mean that to get the best regular timetable, we need to sacrifice train journey time and robustness with a quite large number of overtakings.

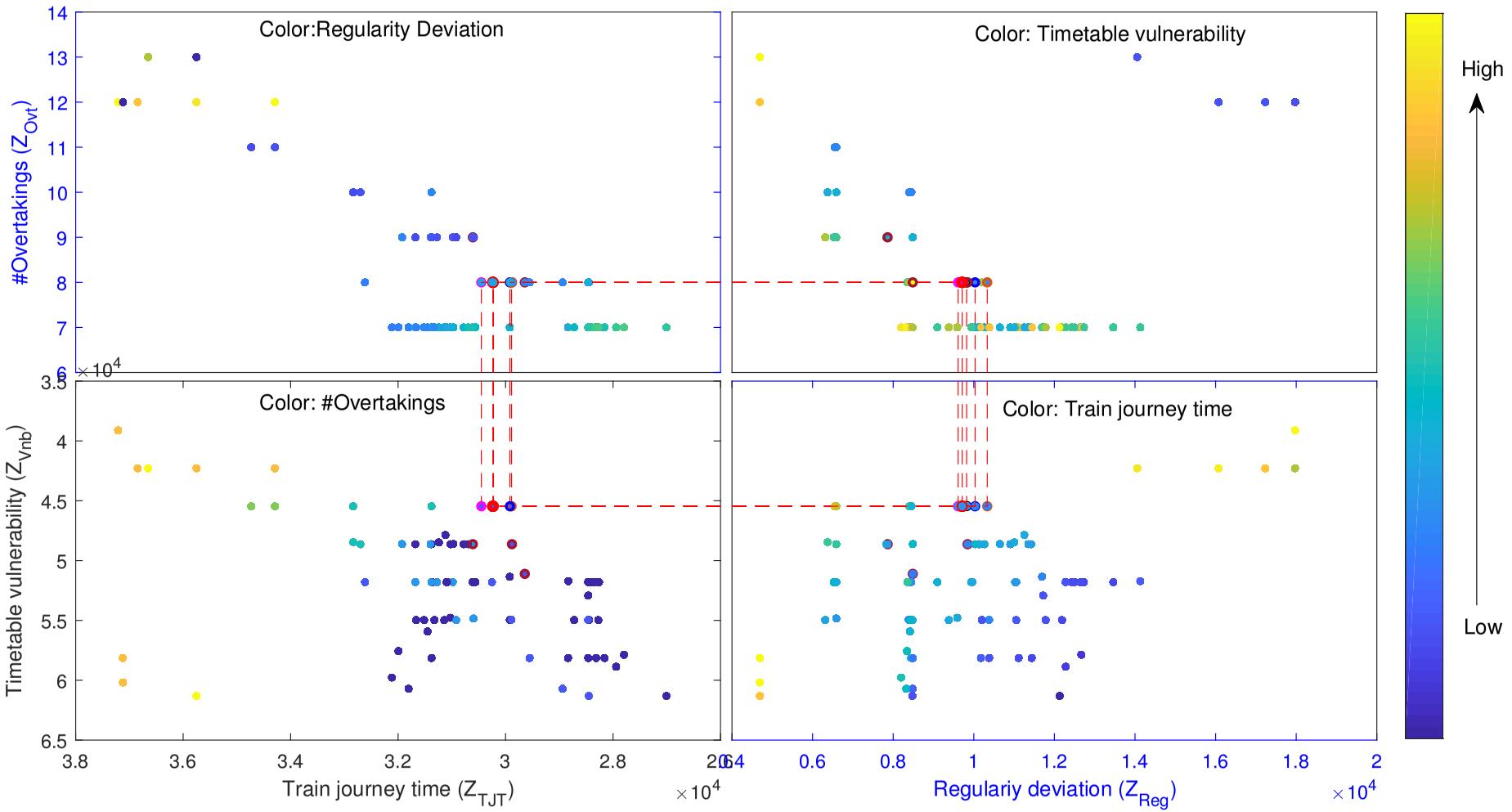

Figure 14: (a) Pareto-optimal set for the MOPRT model in four sub-figures

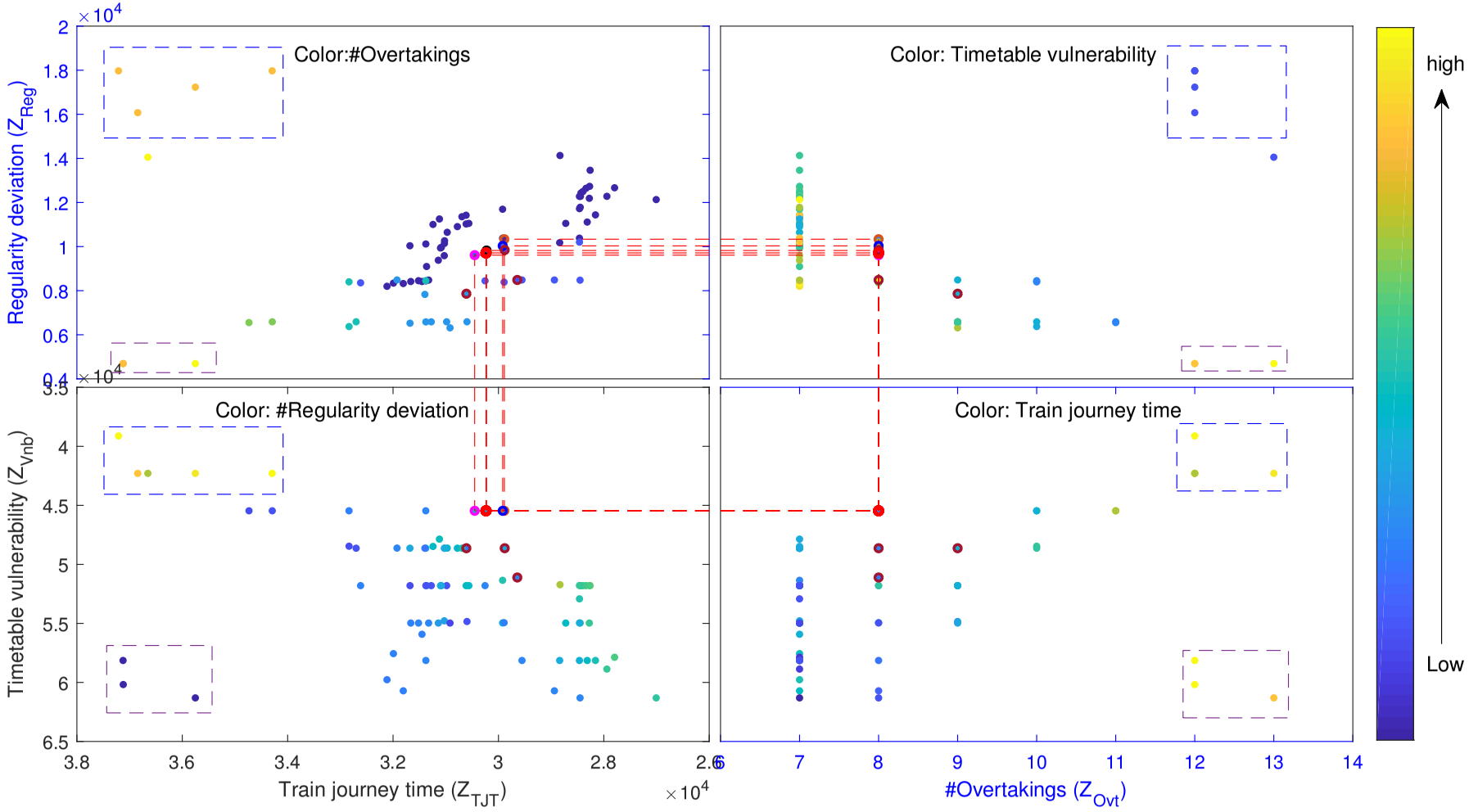

Figure 15: (b) Pareto-optimal set for the MOPRT model in four sub-figures

4.2. Real world instance of a Dutch railway corridor

The Dutch rail network corridor from Utrecht Central (Ut) to Arnhem Central (Ah) is used to test the MOPRT model and solution approach. Figure 16 shows the corridor layout including 10 stations: Utrecht Central, Utrecht Vaartsche Rijn (Utvr), Bunnik (Bnk), Driebergen-Zeist (Db), Maarn (Mrn), Veenendaal-De Klomp (Klp), Ede-Wageningen (Ed), Wolfheze (Wf), Oosterbeek (Otb) and Arnhem Central. The existing line plan and scheduled timetable are shown in Figure 17 and Figure 18, respectively. Basically, ten trains of five lines in each direction follow an hourly train pattern. But IC3000 and S7500 deviate a bit from the basic scheduled train path due to the bi-hourly operation of International train ICE120 when it operates. To set up the model in an hourly pattern, we select the period when all related trains are operating, and use the corresponding line plan as input including the ICE train.

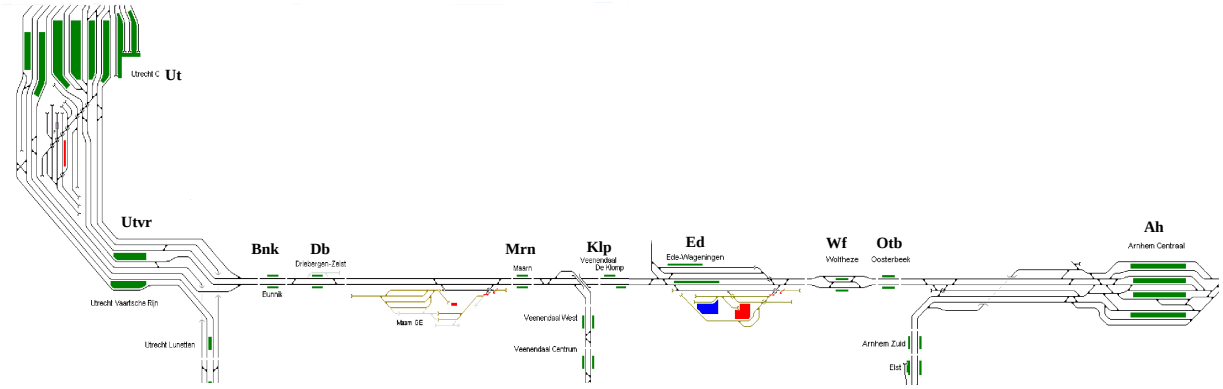

Figure 16: Railway corridor layout from Utrecht Central to Arnhem Central (Source:http://www.sporenplan.nl)

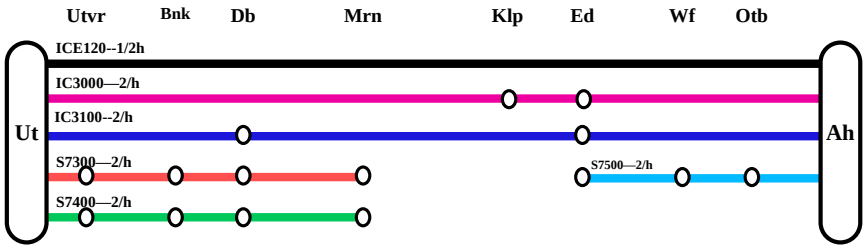

Figure 17: Existing line plan (ICE120 runs once per two hours)

In practice, regularity is always considered between different lines with the same type in a corridor in the Netherlands. Thus, similar to constraint (11), regularity constraints for different lines are also added in our model. To this purpose, Reg_{sl} and Reg_{dl} are defined as the objective values of regularity deviation of the same line and different lines, respectively. To distinguish the importance of regularity deviation from the same line, weights ν_{ij} are proposed for Reg_{sl} and Reg_{dl}. The input parameters for the MOPRT model are listed in Table 7, and the minimum headway between two train activities are depicted in Table 8. Moreover, we applied additional time window constraints to the international ICE train at both boundary stations.

We apply the MOPRT model to find a high-quality timetable for this existing network. First, Table 9 with the initial and updated payoff tables are obtained from the four single-objective models by using Algorithm 1. Both Z_{TJT} and Z_{Vnb} have significant improvements of upper bound. With the achieved minimal and maximal values of Z_{TJT}, Z_{Reg}, and Z_{Vnb}, five grid points are chosen to explore the Pareto frontier. Then, we run Algorithm 2 and Algorithm 3, and 13 Pareto-optimal solutions are found of total 70 feasible solutions, see Table 10. It can be derived that the ε_{TJT} constraint plays the most important role to find the optimal solution as the value of Z_{TJT} is almost the same as ε_{TJT} for most of the solutions. Compared with the regularity deviation, ε_{Vnb} is also restricted better as the objective values Z_{Vnb} are quite close to ε_{Vnb}. Both can be explained by the analysis of Figure 14 and Figure 15 in 4.1.2, there are

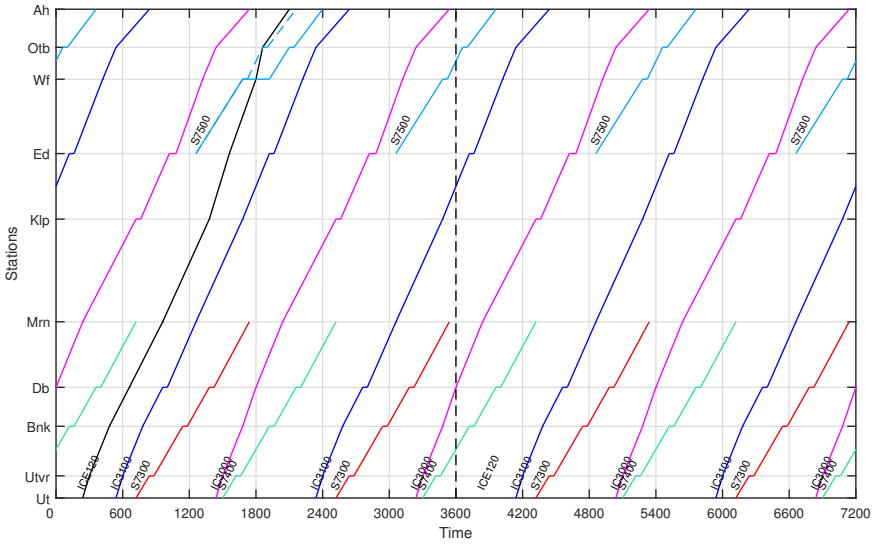

Figure 18: Time-distance diagram of existing scheduled timetable in two hours (Timetable in the second hour is the basic pattern, and the dashed line of S7500 in the first hour indicates that the scheduled train path do not follow the basic pattern due to bi-hourly international train ICE120)

Table 7: Input parameters of MOPRT model

Parameter	Value
Period length T	3600 s
Weight of activity α_{ij}	1 if $(i, j) \in \mathcal{A}_{\text{run}}$, and 3 if $(i, j) \in \mathcal{A}_{\text{dwell}}$
Minimum dwell time	42 s (Sprinter station), 54 s (Intercity station)
Running time supplement	5% (minimum); 20%(maximum)
Maximum dwell time supplement	360 s for stations with one overtaking facility, and 540 s for two
Maximum regularity deviations β_l	300 s
Weight of regularity deviations ν_{ij}	1 (trains from different lines); 2 (trains from the same line)

Table 8: Minimum headways between two train activities (unit: min) (Source: 2018 Network statement from ProRail)

Activity		Activity 2nd train			
		A	P	S	D
Activity 1st train	Arrival(A)	3	2	3	n/a
	Passing(P)	3	3	3	2
	Short stop(S)	3	3	3	3
	Departure(D)	4*	4	3	3

* In case of platform interval.

correlations between overtakings and the train journey time, and overtakings and timetable vulnerability. Even though no overtaking occurs in this solution set, the constraints still work. Meanwhile, the MOPRT model could find the Pareto-optimal solution set in a short time (maximal 5 min but mostly in only a few seconds).

To compare the solutions from the Pareto-optimal set with the existing timetable, we selected six solutions from Table 10: the best obtained timetable (No.1), the best capacity utilization (No.3), the minimal train journey time (No.5), the minimal timetable vulnerability (No.10 and No.12), and the minimal regularity deviation (No.13). These solutions are illustrated in Table 11 together with the existing timetable in the hourly pattern when ICE is running, including values of Z_{TJT}, Z_{Reg}, Z_{Vnb}, Z_{Ovt}, regularity deviation between the same line Reg_{sl}, regularity deviation between different lines Reg_{dl}, minimum cycle time λ, capacity utilization C, and standardized Euclidean distance ρ.

The existing timetable has a quite small regularity deviation between the same line (Reg_{sl}=1584), even smaller

Table 9: Initial (left) and updated (right) payoff table from Algorithm 1

Model/objectives	Initial payoff table				Updated payoff table			
	Z_{TJT} [s]	Z_{Reg} [s]	Z_{Vnb} [s]	Z_{Ovt} [-]	Z_{TJT} [s]	Z_{Reg} [s]	Z_{Vnb} [s]	Z_{Ovt} [-]
PESP-TJT	16902	47360	60930	0	16902	47360	32190	0
PESP-Reg	22667	1036	61900	400	17394	1036	47110	0
PESP-Vnb	19459	64558	13800	0	18486	64552	13800	0
PESP-Ovt	17319	41916	63580	0	17319	41890	21960	0

Table 10: Pareto-optimal solutions for the MOPRT model (sorted according to ρ)

No.	ε_{TJT} [s]	ε_{Reg} [s]	ε_{Vnb} [s]	Z_{TJT} [s]	Z_{Reg} [s]	Z_{Vnb} [s]	Z_{Ovt} [-]	$\widetilde{Z}_{TJT}$ [-]	$\widetilde{Z}_{Reg}$ [-]	$\widetilde{Z}_{Vnb}$ [-]	$\widetilde{Z}_{Ovt}$ [-]	ρ [-]	C [%]	Opt time [s]
1	17694	16915	22128	17694	16904	22120	0	0.5000	0.2498	0.2498	0	0.6122	68.97	55.45
2	17298	16915	30455	17298	16910	30450	0	0.2500	0.2499	0.4998	0	0.6122	73.00	37.99
3	17694	48673	22128	17693	31300	22120	0	0.4994	0.4765	0.2498	0	0.7340	67.69	3.10
4	17298	16915	38783	17298	16158	37410	0	0.2500	0.2381	0.7088	0	0.7884	74.19	3.12
5	16902	16915	38783	16902	16582	38780	0	0.0000	0.2448	0.7499	0	0.7889	81.17	3.62
6	17694	48673	30455	17693	27120	29540	0	0.4994	0.4107	0.4725	0	0.8008	68.11	2.61
7	18090	16915	22128	18090	15690	22120	0	0.7500	0.2307	0.2498	0	0.8235	68.58	114.97
8	17298	48673	22128	17298	48370	22120	0	0.2500	0.7452	0.2498	0	0.8248	72.64	260.96
9	18486	16915	30455	17878	16060	30450	0	0.6162	0.2365	0.4998	0	0.8279	72.83	2.64
10	18090	32794	22128	18090	32792	22110	0	0.7500	0.5000	0.2495	0	0.9353	67.92	10.93
11	17298	48673	38783	17297	38608	38770	0	0.2494	0.5915	0.7496	0	0.9869	77.53	3.34
12	18090	48673	22128	18012	48660	22110	0	0.7008	0.7498	0.2495	0	1.0562	69.69	2.43
13	18090	16915	47110	18090	11524	44890	0	0.7500	0.1651	0.9334	0	1.2087	70.25	1.67

than the best regularity solution No.13 with 2924. Whereas it has a larger regularity deviation between different lines (Reg_{dl}=8664) comparing with solutions No.1 (7376), No.5 (8398) and No.13 (5676). More importantly, the existing timetable also has the largest timetable vulnerability (65380) and capacity utilization (84.67%), both of which are larger than the worst solution in our Pareto-optimal set. The minimal and maximal timetable vulnerability is 22110 and 44890 respectively, which are much smaller than the existing one (existing one is around three times larger than our best timetable vulnerability solutions No.10 and No.12). This indicates that this timetable could be easily affected by delays and it is difficult to schedule more trains. Moreover, the existing timetable also has a larger train journey time Z_{TJT}=18564 than all obtained timetables. One reason that the existing timetable has longer train journey times is that an overtaking occurs in the timetable, while no overtaking occurs in any of our solutions. Meanwhile, the capacity utilization of our solutions are all better than the existing timetable that actually violates the UIC capacity norm. Therefore we found timetables that scored better on all criteria and used the capacity much better. Also note that the overtaking in the existing timetable is not designed very well as it disturbs an existing train service when the ICE is running while the overall capacity utilization did not improve. Hence, our solution could provide timetables with less travel time and better capacity utilization, attracting more passengers. It can be observed that our solution No.13 is better than the existing timetable for all four objectives. The best calculated solution No.1 has 4.69% decrease of train journey time, 66.17% decrease of timetable vulnerability, 18.54% reduction of capacity utilization, but a regularity deviation with an increase of 42.87%. The time-distance diagram is displayed in Figure 19. Note also that train orders are significantly different compared to the existing timetable from Figure 17. Above all, these results demonstrate that our MOPRT model and algorithms could effectively provide high-quality timetables for railway corridors. In practice, different timetables are necessary in different situations for a network. Our multi-objective approach supports the planners to choose from the Pareto optimal solutions .

Table 11: Comparison between existing timetable with timetables from the Pareto-optimal set

Timetables	Z_{TJT} [s]	Z_{Reg} [s]	Z_{Vnb} [s]	Z_{Ovt} [-]	Reg_{sl} [s]	Reg_{dl} [s]	λ [s]	C [%]	ρ [-]
Existing timetable	18564	11832	65380	1	1584	8664	3048	84.67	-*
No.1 (best ρ)	17694	16904	22120	0	4764	7376	2483	68.97	0.6122
No.3 (capacity utilization)	17693	31300	22120	0	9218	12864	2437	67.69	0.7340
No.5 (train journey time)	16902	16582	38780	0	4092	8398	2922	81.17	0.7889
No.10 (timetable vulnerability)	18090	32792	22110	0	9766	13260	2445	67.92	0.9353
No.12 (timetable vulnerability)	18012	48660	22110	0	18790	11080	2509	69.69	1.0562
No.13 (timetable regularity)	18090	11524	44890	0	2924	5676	2529	70.25	1.2087

* Value of Z_{Vnb} from the existing timetable exceed the range from the case.

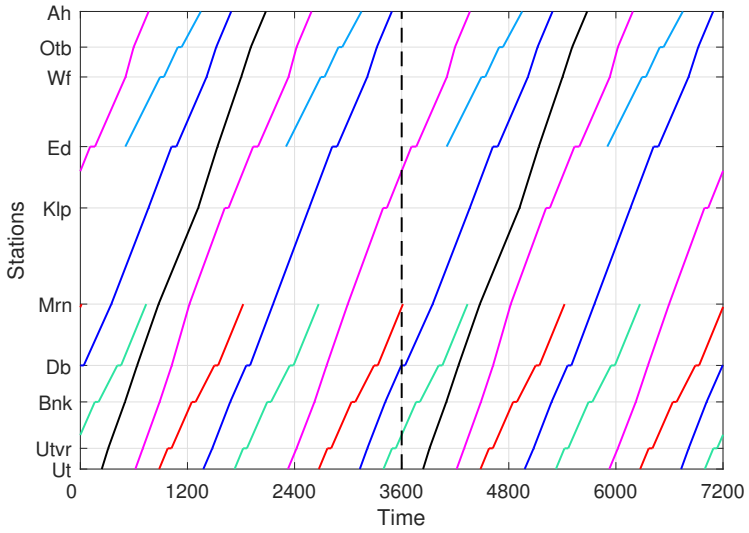

Figure 19: Time-distance diagram of the optimal timetable from the Pareto-optimal set

4.3. Comparison of the flexible overtaking models in this paper and in the literature

To demonstrate the efficiency of our designed flexible overtaking model with multiple overtakings in Section 2.2.4, we compare the solution with the original single flexible overtaking constraints from Zhang and Nie (2016). The theoretical instance in Section 4.1 is chosen as a prototype of a dense heterogeneous corridor. Modified with two types of flexible overtaking constraints, the four single-objective timetabling models (PESP-TJT, PESP-Reg, PESP-Vnb and PESP-Ovt) are applied. To be specific, single flexible overtaking constraints and multiple overtakings constraints are added respectively to each model to compute the solutions, shown in Table 12. It can be observed that all optimal values of each single-objective model with our multiple overtakings constraints are better than the original single one, with 5.28% decreased train journey time, 62.90% decreased timetable regularity deviation, 29.13% decreased timetable vulnerability, and 2 reduced overtakings. Furthermore, the capacity utilization in the four scenarios with our flexible overtakings constraints are still lower, even for the one with fewer overtakings in the timetable from PESP-Ovt. This demonstrates that our designed multiple overtaking constraints in the flexible overtaking model are more efficient than the original single overtaking constraints.

5. Conclusions

The rail system becomes more and more complex, and different performance indicators need to be taken into account during the timetabling process. Accordingly, the single-objective optimization models become difficult to

Table 12: Optimization results of the four modified single-objective models with two different types of flexible overtaking constraints

Models	Single flexible overtaking constraints		Multiple overtakings constraints	
	Optimal value	Capacity utilization	Optimal value	Capacity utilization
PESP-TJT	28512	93.33%	27006	90.67%
PESP-Reg	12684	93.33%	4692	83.00%
PESP-Vnb	55200	93.33%	39120	83.56%
PESP-Ovt	9	93.33%	7	92.64%

find high-quality timetables considering multiple indicators. Therefore, this paper proposed a new multi-objective periodic railway timetabling (MOPRT) model and solution approach.

The MOPRT model consists of the four objectives train journey time, timetable regularity deviation, timetable vulnerability, and the number of overtakings, and four corresponding single-objective models PESP-TJT, PESP-Reg, PESP-Vnb, and PESP-Ovt are introduced. To deal with the multiple objectives, the ε-constraint method is applied and three algorithms are designed to efficiently create the Pareto frontier. Algorithm 1 computes tight lower and upper bounds for each objective to narrow down the range. Algorithm 2 explores the model feasibility space with given ε-constraints. Algorithm 3 generates the Pareto-optimal solution set. Both Algorithm 1 and Algorithm 2 are designed to reduce the number of computations in Algorithm 3.

We tested the proposed MOPRT model and solution approach in two instances, a theoretical instance and a real-world instance. The theoretical instance demonstrated that each single-objective model is effective in finding the optimal solution of the corresponding objective and three designed algorithms perform well to generate the Pareto Frontier. Algorithm 1 and Algorithm 2 effectively reduced the number of unnecessary solutions and thus significantly reduced the computation times. From the trade-off analysis of the computation results, it was observed that the number of overtakings has a negative impact on timetable vulnerability and a positive effect on timetable capacity. To be specific, more overtakings could help to improve timetable robustness and reduce capacity utilization for a dense railway traffic system. The experiments on the real-world case of the Dutch railway corridor showed that our model can find better solutions than the existing timetable for the objectives of train journey time, timetable robustness (according to timetable vulnerability values) and capacity utilization, at the cost of timetable regularity. The best achieved solution from the Pareto-optimal set has 4.69% decrease of train journey time, 66.17% increase of timetable robustness, and 18.54% reduction of capacity utilization.

The computed solutions in the Pareto-optimal set have different objective preferences, which provides more options for the railway planners to choose from when designing a timetable. When the demand increases, a timetable with the best capacity utilization could also be found. If trains adhere well to their scheduled paths then robustness is less an issue and the MOPRT model can prioritize short train journey times, while keeping the other objectives as good as possible. If delays often occur in the corridor, this model could provide the timetable with the best allocation of buffer times at stations, while maintaining the requirements of train journey time and regularity. This way, the MOPRT model provides flexible decision support to timetable planners. This work assumed a given line plan. The integration between line planning and timetabling is another interesting topic with consideration of passenger demand, see e.g. Yan and Goverde (2019).

The nearly saturated capacity utilization of existing railway networks is an urgent issue to be solved. We showed that the number of overtakings has a positive impact on timetable capacity. A direction of future research is to optimize the location and number of new overtaking facilities when the infrastructure does not allow high quality timetables for further increasing frequencies. Hence, our future research will extend the model to finding optimal stations for new overtaking facilities with consideration of train journey time, timetable regularity, investment cost and capacity utilization.

Acknowledgement

This work was partially supported by the China Scholarship Council CSC (No.201309110101). Special thanks to Gerben Scheepmaker and NS who provided the timetable data of the Dutch railway corridor. Besides, the previous version of this paper won the first place in the 2018 INFORMS Railway Applications Section Student Paper Contest.

References

Bešinović, N., 2017. Integrated capacity assessment and timetabling models for dense railway networks. PhD thesis, Delft University of Technology.

Bešinović, N., Goverde, R. M. P., Quaglietta, E., Roberti, R., 2016. An integrated micro–macro approach to robust railway timetabling. Transportation Research Part B: Methodological 87, 14–32.

Binder, S., Maknoon, Y., Bierlaire, M., 2017. The multi-objective railway timetable rescheduling problem. Transportation Research Part C: Emerging Technologies 78, 78–94.

Burdett, R. L., 2015. Multi-objective models and techniques for analysing the absolute capacity of railway networks. European Journal of Operational Research 245 (2), 489–505.

Caimi, G., Kroon, L., Liebchen, C., 2017. Models for railway timetable optimization: Applicability and applications in practice. Journal of Rail Transport Planning & Management 6 (4), 285–312.

Goverde, R. M. P., 2007. Railway timetable stability analysis using max-plus system theory. Transportation Research Part B: Methodological 41 (2), 179–201.

Goverde, R. M. P., Bešinović, N., Binder, A., Cacchiani, V., Quaglietta, E., Roberti, R., Toth, P., 2016. A three-level framework for performance-based railway timetabling. Transportation Research Part C: Emerging Technologies 67, 62–83.

Goverde, R. M. P., Hansen, I. A., 2013. Performance indicators for railway timetables. In: Intelligent Rail Transportation (ICIRT), 2013 IEEE International Conference on. pp. 301–306.

Kroon, L., Maróti, G., Helmrich, M. R., Vromans, M., Dekker, R., 2008. Stochastic improvement of cyclic railway timetables. Transportation Research Part B: Methodological 42 (6), 553–570.

Kroon, L. G., Peeters, L. W., 2003. A variable trip time model for cyclic railway timetabling. Transportation Science 37 (2), 198–212.

Liebchen, C., 2007. Periodic timetable optimization in public transport. In: Waldmann, K.-H., Stocker, U. M. (Eds.), Operations Research Proceedings 2006. Springer, pp. 29–36.

Liebchen, C., Lübbecke, M., Möhring, R., Stiller, S., 2009. The concept of recoverable robustness, linear programming recovery, and railway applications. In: Ahuja, R. K., Möhring, R. H., Zaroliagis, C. D. (Eds.), Robust and online large-scale optimization: Models and Techniques for Transportation Systems. Springer, pp. 1–27.

Liebchen, C., Möhring, R. H., 2007. The modeling power of the periodic event scheduling problem: railway timetables-and beyond. In: Geraets, F., Kroon, L., Schoebel, A., Wagner, D., Zaroliagis, C. D. (Eds.), Algorithmic methods for railway optimization. Springer, pp. 3–40.

Löfberg, J., 2004. Yalmip : A toolbox for modeling and optimization in matlab. In: In Proceedings of the CACSD Conference. Taipei, Taiwan.

Lusby, R. M., Larsen, J., Bull, S., 2018. A survey on robustness in railway planning. European Journal of Operational Research 266 (1), 1–15.

Marler, R. T., Arora, J. S., 2004. Survey of multi-objective optimization methods for engineering. Structural and multidisciplinary optimization 26 (6), 369–395.

Maróti, G., 2017. A branch-and-bound approach for robust railway timetabling. Public Transport 9 (1-2), 73–94.

Mavrotas, G., 2009. Effective implementation of the ε-constraint method in multi-objective mathematical programming problems. Applied mathematics and computation 213 (2), 455–465.

Mavrotas, G., Florios, K., 2013. An improved version of the augmented ε-constraint method (AUGMECON2) for finding the exact pareto set in multi-objective integer programming problems. Applied Mathematics and Computation 219 (18), 9652–9669.

Nachtigall, K., 1996. Periodic network optimization with different arc frequencies. Discrete Applied Mathematics 69 (1), 1–17.

Parbo, J., Nielsen, O. A., Prato, C. G., 2016. Passenger perspectives in railway timetabling: a literature review. Transport Reviews 36 (4), 500–526.

Peeters, L., 2003. Cyclic railway timetable optimization. PhD thesis, Erasmus University Rotterdam.

Sels, P., Dewilde, T., Cattrysse, D., Vansteenwegen, P., 2016. Reducing the passenger travel time in practice by the automated construction of a robust railway timetable. Transportation Research Part B: Methodological 84, 124–156.

Serafini, P., Ukovich, W., 1989. A mathematical model for periodic scheduling problems. SIAM Journal on Discrete Mathematics 2 (4), 550–581.

Sparing, D., Goverde, R. M. P., 2017. A cycle time optimization model for generating stable periodic railway timetables. Transportation Research Part B: Methodological 98, 198–223.

UIC, 2013. Code 406: capacity, second edition. Pairs: International Union of Railways.

Wardman, M., Shires, J., Lythgoe, W., Tyler, J., 2004. Consumer benefits and demand impacts of regular train timetables. International Journal of Transport Management 2 (1), 39–49.

Yan, F., Goverde, R. M. P., 2017. Railway timetable optimization considering robustness and overtakings. In: 2017 5th IEEE International Conference on Models and Technologies for Intelligent Transportation Systems (MT-ITS). pp. 291–296.

Yan, F., Goverde, R. M. P., 2019. Combined line planning and train timetabling for strongly heterogeneous railway lines with direct connections. Transportation Research Part B: Methodological, under review.

Zhang, X., Nie, L., 2016. Integrating capacity analysis with high-speed railway timetabling: A minimum cycle time calculation model with flexible overtaking constraints and intelligent enumeration. Transportation Research Part C: Emerging Technologies 68, 509–531.